博士學位論文

Synthesis and Characterization of Chromium(III) Complexes with 14-Membered Tetraaza Macrocycle and O- or N-donor Auxiliary Ligands

濟州大學校 大學院
化學科
金 九 哲

2003年 12月

Synthesis and Characterization of Chromium(III) Complexes with 14-Membered Tetraaza Macrocycle and O- or N-donor Auxiliary Ligands

Goo-Cheol Kim

(Supervised by professor Jong-Chul Byun)

A thesis submitted in partial fulfillment of the requirement for the degree of Doctor of Philosophy.

2003. 12. .

This thesis has been examined and approved.

Date Approved :

Department of Chemistry
GRADUATE SCHOOL
CHEJU NATIONAL UNIVERSITY

Contents

List of Tables

List of Figures

Abstract

The reaction of *cis*-$[Cr([14]\text{-decane})(OH_2)_2]^+$ ([14]-decane = *rac*-5, 5, 7, 12, 12, 14-hexamethyl-1, 4, 8, 11-teraazacyclotetradecane) with O- {L_a : chloroacetate (ca), benzoate (bz), *p*-chlorobenzoate (cbz), oxalate (ox), malonate (mal), acetylacetonate (acac), citrate (cit)} or N- {L_a : NCS^-, N_3^-} bonded auxiliary ligands formed a new *cis*-$[Cr(III)([14]\text{-decane})(L_a)_m]^{n+}$ complexes. These complexes have been characterized by a combination of elemental analysis, conductivity, IR and Vis spectroscopy, mass spectrometry, thermogravimetry, and X-ray crystallography. The crystal structures of four complexes were determined by X-ray crystallography. The complexes have been showed a distorted octahedral coordination environment with the macrocycle adopting a folded *cis*-V conformation. The crystal of *cis*-$[Cr([14]\text{-decane})(NCS)_2]ClO_4 \cdot H_2O$ was orthorhombic, space group *Pbca*, with cell constant a=15.295Å, b=16.4850(10)Å, c=21.0490(10)Å, α=90°, β=90°, γ=90°, V=5307.3(4)$Å^3$, and Z=8. The hexacoordination geometry around Cr^{3+} ion exhibited a distorted octahedral structure. In this complex Cr(III) was coordinated with the four secondary nitrogen atoms of the macrocycle and two nitrogen atom of two

isothiocyanate in the *cis* position. The crystal of *cis*-[Cr([14]-decane)(cbz)$_2$]ClO$_4$ was orthorhombic, space group *Pbca*, with cell constant *a*=12.0930(10)Å, *b*=20.3580(10)Å, *c*=28.852Å, α=90°, β=90°, γ=90°, *V*=7103.1(7)Å^3, and *Z*=8. The hexacoordination geometry around Cr(III) ion was a distorted octahedral in which Cr(III) was coordinated with the four secondary nitrogen atoms of the macrocycle as well as with two oxygen atom of two chlorobezoate in the *cis* position. The crystal of *cis*-[Cr([14]-decane)(acac)](ClO$_4$)$_2$·0.5H$_2$O was monoclinic, space group C2/c, with cell constant *a*=20.0210(10)Å, *b*=30.1120(10)Å, *c*=12.708Å, α=90°, β=127.2170(10)°, γ=90°, *V*=6101.4(4)Å^3, and *Z*=8. The hexacoordination geometry around Cr(III) ion was a distorted octahedral in which Cr(III) was coordinated with the four secondary nitrogen atoms of the macrocycle as well as with two oxygen atom of bidentated acethylacetone(acac) in the *cis* position. The crystal of *cis*-[{Cr([14]-decane)(μ-cit)}$_2$](ClO$_4$)$_2$·6H$_2$O was monoclinic, space group C2/c, with cell constant *a*=23.818(2)Å, *b*=21.139(2)Å, *c*=16.1350(10)Å, α=90°, β=127.294(4)°, γ=90°, *V*=6462.8(9)Å^3, and *Z*=8. The structure of the cation in citrato complex revealed two identical homobinuclear Cr(III)Cr(III) cores joined by two bridging citrato group linkage. The cation was centro-symmetric. The hexacoordination geometry around Cr(III) ion was a distorted octahedral in which Cr(III) was coordinated with the four secondary nitrogen atoms of the macrocycle as well as with two oxygen atom of two monodentated citrate in the *cis* position. The distence between two Cr metal ions was 7.360Å. The visible absorption spectra of *cis*-$[Cr([14]\text{-decane})(L_a)_m]^{n+}$ in DMF solution at room temperature exhibited two bands, at 17400~18800 $cm^{-1}(\nu_1)$ and 23400~25900 $cm^{-1}(\nu_2)$, due to the $^4A_{2g} \rightarrow {}^4T_{2g}$ and $^4A_{2g} \rightarrow {}^4T_{1g}$ (O_h) transitions, respectively. The FAB mass spectra peaks of all complexes were corresponding to the molecular ion $[Cr([14]\text{-decane})(L_a)_m]^+$ (m = 1 or 2). Thermogravimetry analysis(TGA) for the Cr(III) complexes was found out from the results that the prepared macrocycle compounds have relatively high thermal stability. The macrocyclic entity changed slowly up to 350℃, and then those complexes have been changed to green Cr_2O_3 were observed at over 990℃.

I. Introduction

Intensive studies on coordination chemistry of macrocyclic multidentate ligands have led to useful approaches towards ligand design for selective complexation of metal ions.[1-3] The macrocyclic ligand has two specific properties; ring size effect and macrocyclic effect. The former means that macrocyclic ligand can select the metal ion whose ionic radius fits the ligand cavity size. The latter describes the significant enhancement in complex stability constants in the appropriately fitted macrocyclic ligands compared to their open-chain analogues.[4, 5]

Both the ring size and macrocyclic effect have been extensively examined in the view point of thermodynamics.[6-9] Selectivity patterns can be tested with the combined effects of (1) metal ion solvation, (2) ligand solvation, and (3) ligand conformation.[6, 10] Thöm and co-workers have been examined this hole-size selectivity with a nitrogen-donor tetra-aza macrocycle.[11] The hole-size has been estimated using molecular mechanics calculation for the several macrocyclic ligands.[12]

Among pyridinocrown ethers[1] of different ring sizes (from 15-crown-5 to 33-crown-11), the ligand with 18-membered ring exhibits the maximum binding constants for all alkali metal cations.[13] Several pyridino macrocycles showed more effective membrane carriers for Ag^+ than the parent crown ethers.[14] Kumar, Singh and co-workers synthesized a series of pyridine-containing macrocycles and characterized their metal ion complexation properties.[15]

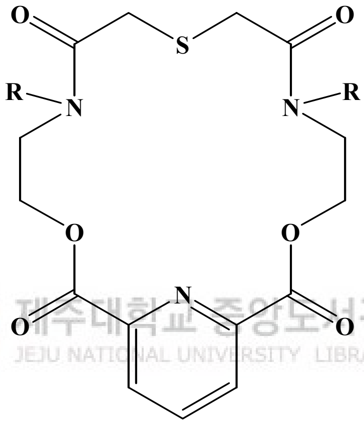

[1]

Recently the interest in polyazamacrocyclic chelate compounds with paramagnetic and radioactive metal ion has grown considerably, largely due to their biomedical applications such as (1) magnetic resonance imaging(MRI) contrast agents,[16, 17] (2) NMR shift-relaxation probes of the dynamic solution conformation of molecules, (3) shift reagents for NMR-active cations,[18] and (4) diagnostic and therapeutic radiopharmaceuticals.[19] Consequently the investigations of macrocyclic complexes by electrochemical, spectral, structural, kinetic and thermodynamic evaluations has received considerable attention. As a result of these studies, a number of paramagnetic metal chelates are using clinical agents as bioconjugates for monoclonal antibody radioisotope labeling and MRI contrast agents.

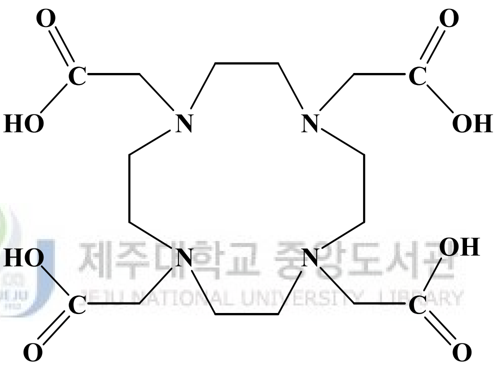

[2]

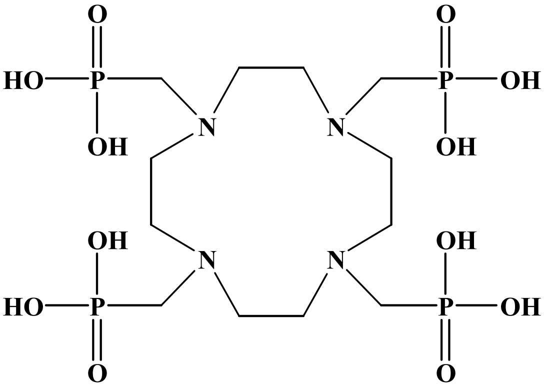

[3]

A ligand, DOTA (1, 4, 7, 10-tetraazacyclododecane-*N*, *N*′, *N*′′, *N*′′′-tetraacetate)[2], derived from tetraazacyclododecane (cyclen) forms one of the most thermodynamically stable and kinetically inert complexes with the trivalent lanthanide cations.[20] Due to the positive properties, $[Gd(DOTA)]^-$ is one of the most effective and safest MRI contrast enhancement agents.[21] The complex formed from lanthanide metals and the methylenephosphonate analog, DOTP (1, 4, 7, 10-tetraazacyclododecane-*N*, *N*′, *N*′′, *N*′′′-tetrakis(methylene-phosphonate))[3], has also been examined in some detail.[22] For example, Tm^{3+}complex, $[Tm(DOTP)]^{5-}$ is proven to be a versatile $^{23}Na^+$ shift agent, for both perfused tissues and *in vivo* animal studies.

Since the importances of axial coordination in transition metal-macrocyclic complexes in their biological functions, the reactivity of metal complexes toward Lewis base like CO, *N*-methylimidazole has been studied extensively.[23, 24]

Studies on the interaction between cyanide anions and Co(Ⅲ) complexes are important not only in coordination chemistry but also in toxicology. Because of the high affinity of CN^- anions for cobalt complexes, hydroxocobalamin[25, 26] and water-soluble Co(Ⅲ) porphyrins[27] have been investigated as an effective antidote to the lethal effects of cyanide anions. The mechanism of the detoxification clearly involves the formation of cyanide complex.

This thesis deals with the syntheses (Scheme 1), characterization and crystal structures of *cis*-[Cr(III)([14]-decane)$(L_a)_m]^{n+}$ ([14]-decane ; 5, 5, 7, 12, 12, 14-hexamethyl-1, 4, 8, 11-tetraazacyclotetradecane) complexes containing O- or N-bonded auxiliary ligands {L_a : NCS^-, N_3^-, chloroacetate (ca ; $ClCH_2COO^-$), benzoate (bz ; $C_6H_5COO^-$), *p*-chlorobenzoate (cbz ; $ClC_6H_4COO^-$), oxalate (ox ; $^-OOCCOO^-$), malonate (mal ; $^-OOCCH_2COO^-$), acetylacetonate (acac ; $CH_3COCHCOCH_3^-$), citrate (cit ; $^-OOCCH_2C(OH)(COO^-)CH_2COOH$), } at the *cis* positions.

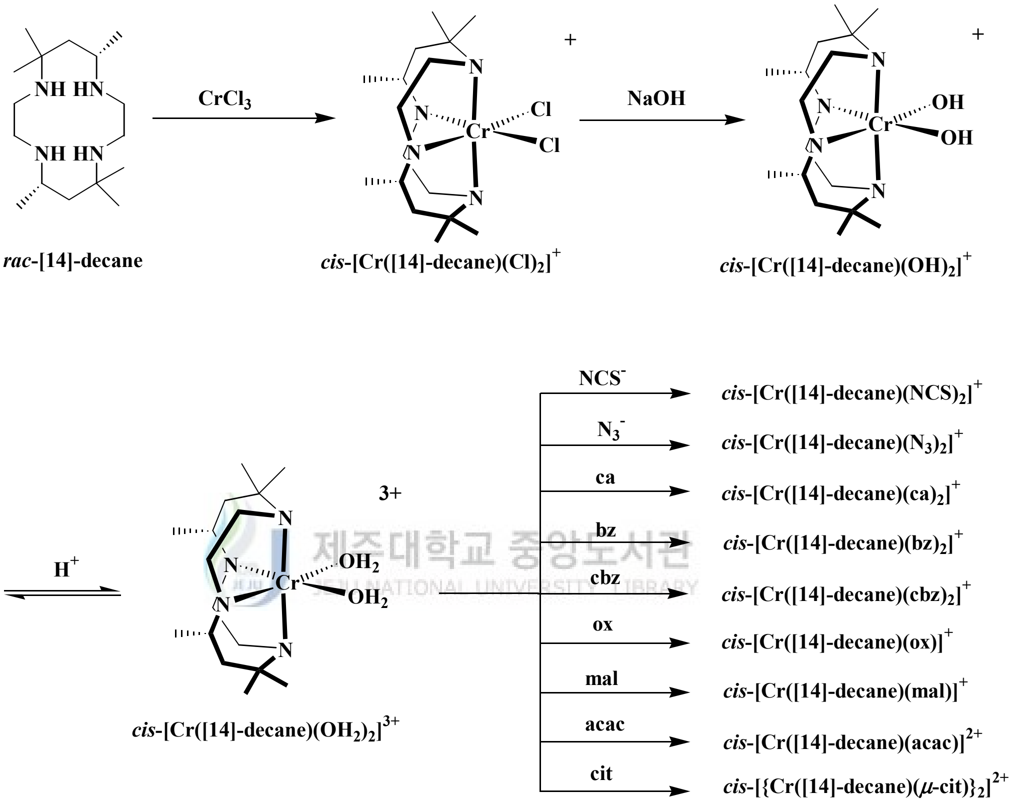

Scheme 1. Syntheses of the *cis*-$[\mathrm{Cr}([14]\text{-decane})(\mathrm{L_a})_m]^{n+}$($m$, n : 1 or 2).

II. Experimental Section

1. Materials

In synthesis of macrocyclic ligand, ethylenediamine, acetone, $HClO_4$, NaOH and $NaBH_4$ purchased from by Junsei Chemical Co without further purification. All other materials and solvents in synthesis of complexes were used as purchased from Aldrich-Sigma or Fisher. *rac*-[14]-Decane macrocyclic ligand, *cis*-$[Cr([14]\text{-decane})(Cl)_2]Cl$ and *cis*-$[Cr([14]\text{ -decane})(OH)_2]^+$ solution were prepared according to the literatures.[28, 29]

2. Physical Measurements

Microanalyses of C, H, and N were carried out using LECO CHN-900 analyzer. The electronic absorption spectra of the complexes were acquired 700-300 nm at 25℃ by using a HP model 8453 UV-VIS spectrophotometer. The measurement sample of complexes were prepared with DMF and a matched pair of Teflon stopped quartz cells were used. Conductivity measurements of the complexes were carried out at 25 ± 1℃ in DMF using an ORION 162 conductivity temperature meter. IR spectra were recorded on a Bruker FSS66 FT-IR spectrometer in the range 4000-370 cm^{-1} using KBr pellets. FAB-mass spectra were obtained on a JEOL JMS-700 mass spectrometer(6 kV, 10 mA) using argon as the FAB gas. The accelerating voltage was 10kV and spectra were recorded at room temperature. Glycerol was used as the matrix. The mass spectrometer was operated in positive ion mode, and mass spectum was calibrated by Alkali-CsI positive. TGA were carried out on a TGA 2050 thermal analyzer. The thermogravimetric curves of complexes were recorded in 30～1000℃ range in nitrogen atmosphere. The heating rate was 5℃/min, but 1℃/min in 250～350℃ range.

3. Synthesis of Ligands

1) 5, 5, 7, 12, 12, 14-Hexamethyl-1, 4, 8, 11-tetraazacyclotetradeca-4, 11-diene (*trans*-[14]-diene) diperchlorate

Ethylenediamine(2.03 mL, 30 mmol) and concentrated $HClO_4$ (8.16 mL, 75 mmol) were added dropwise in aceton (45 mL). The mixture was heated at 45℃ with stirring for *ca.* 30min. Afterwards ethylenediamine (2.03 mL, 30 mmol) and 45 mL acetone were added into the mixture then heated at 45℃ with stirring for *ca.* 24 h. The mixture was cooled to room temperature. The white precipitate was removed by filteration, washed with ice-cold acetone, then dried under vacuum.

Yield 71%.

Anal. Calcd (Found, %) $C_{16}H_{38}N_4$,$2HClO_4$ (Fw. 481)

C, 39.99 (39.92) : H, 7.11 (7.07) : N, 11.43 (11.64).

^{1}H-NMR (400 MHz, $CDCl_3$)

δ (ppm) 1.30 (12H, $C(CH_3)_2$), 1.92 (6H, CCH_3)
2.62 (4H, CH_2), 3.23 (4H, $HNCH_2$)
3.45 (4H, NCH_2), 8.54 (2H, NH)

^{13}C-NMR (100 MHz, $CDCl_3$)

δ (ppm) 21.24, 24.44, 42.30, 43.59, 47.26, 58.18, 174.70

m.p. 107～108℃

2) 5, 5, 7, 12, 12, 14-hexamethyl-1, 4, 8, 11-tetraazacyclotetra-decane(*rac*-[14]-decane)

trans-[14]-Diene diperchlorate(10 g, 21 mmol) was dissolved in methanol (50 mL). Sodium borohydride (1.9 g, 63 mmol) and sodium hydroxide (1.65 g, 40 mmol) were added alternatively in small portions to warmed solution for 1 h. The solution was stirred at room temperature for 1h, and refluxed for 15 min. Sodium hydroxide aqueous solution(5 g in 100 mL water) was added in the solution, and stirred for 1 h. The white precipitate was removed by filteration and washed with ice-cold water then dried under vacuum.

The methanol(ca. 60 mL) solution was refluxed until all precipitate dissolved. The resulting solution was filtered off when it was hot. The filtrate was added into water (40 mL), and cooled in ice-bath. Fine crystals of *meso*-[14]-decane were slowly formed. The product was removed by filteration and washed with water.

Potassium hydroxide (*ca.* 10 g) was added to the remained aqueous filtrate of the previous procedure with stirring. The product (*rac*-[14]-decane) was removed by filteration and recrystallised from dry ether then dried under vacuum.

Yield 2.10 g (33%).
Anal. Calcd (Found, %) $C_{16}H_{36}N_4,H_2O$ (Fw. 302.50)
C, 63.53 (63.50) : H, 12.66 (12.70) : N, 18.52 (18.50).
^1H-NMR (400 MHz, $CDCl_3$)
δ (ppm) 1.09 (12H, $C(CH_3)_2$), 0.95 (6H, CCH_3)
^{13}C-NMR (100 MHz, $CDCl_3$)
δ (ppm) 21.26, 28.33, 29.41, 41.15, 43.59, 48.09, 51.47, 52.61
FAB-mass : m/z 303 ($C_{16}H_{36}N_4,H_2O$)
m.p. 101～108℃

4. Synthesis of Complexes

1) *cis*-[Cr([14]-decane)$(Cl)_2$]Cl

cis-[Cr([14]-decane)$(Cl)_2$]Cl complex was prepared by the reaction of $CrCl_3$, Zn powder, and *rac*-5, 5, 7, 12, 12, 14- hexamethyl -1, 4, 8, 11-tetraazacyclotetradecane(*rac*-[14]-decane) hydrate according to the literature. $CrCl_3$ (10 g) was dissolved in 50 mL *N*-methyl

-formamide with Zn powder (*ca.* 10 mg). The *rac*-[14]-decane ligand (18 g) was added into the resulting solution, then refluxed for 2 h. A bluish-green precipitate was slowly formed during this treatment. The resulting mixture was cooled in ice-bath. The precipitate was removed by filteration and washed twice with cold-water and ethanol then dried under vacuum.

Anal. Calcd (Found, %) $C_{16}H_{38}N_4Cl_3Cr$ (442.35)
C, 43.40 (43.60) : H, 8.14 (8.30) : N, 12.66 (12.51).

2) *cis*-$[Cr([14]\text{-decane})(OH)_2]^+$ solution

cis-$[Cr([14]\text{-decane})(OH)_2]^+$ solution was prepared by dissolving *cis*-$[Cr([14]\text{-decane})(Cl)_2]Cl$ in NaOH aqueous solution according to the literatures. *cis*-$[Cr([14]\text{-decane})(Cl)_2]Cl$ (10 g) was dissolved in the NaOH aqueous solution (4 g NaOH in 100 mL water) at 100℃. The resulting blue-colored solution was cooled to room temperature and filtered off the residues of undissolved material. This solution was as the starting material for the following preparations.

3) *cis*-$[Cr([14]\text{-decane})(OH)_2]ClO_4 \cdot 3H_2O$

The saturated $NaClO_4$ solution (2 mL) was slowly added to *cis*-$[Cr([14]\text{-decane})(OH)_2]^+$ solution (2 mmol, 10 mL). The mixture was stirred 1 h, then cooled in ice bath. The bluish-black crystals were removed by filteration and washed twice with ice-cold acetone quickly, then dried under vacuum.

Yield 78%.

Anal. Calcd (Found, %) $C_{16}H_{38}N_4O_6ClCr \cdot 3H_2O$ (Fw. 523.99)

C, 36.68 (36.55): H, 8.46 (8.25): N, 10.69 (10.34).

UV/Vis. (in DMF)

λ_{627nm} (ε=106 M^{-1} cm^{-1}), λ_{383nm} (ε=157.5 $M^{-1}cm^{-1}$).

Λ_M (in DMF) : 71.4 ohm^{-1} cm^2 mol^{-1}.

4) *cis*-$[Cr([14]\text{-decane})(NCS)_2]ClO_4 \cdot H_2O$.

cis-$[Cr([14]\text{-decane})(OH)_2]^+$ solution (2 mmol, 10 mL) was acidified with the aqueous solution of $HClO_4$(70%, *ca.* 1mL). The resulting solution was mixed with the aqueous solution of NaSCN (0.83 g in 50 mL water). Then saturated $NaClO_4$ solution (4 mL) was added into the previous mixture. The resulting mixture was stirred 4 h at room temperature. The product acquired as pink precipitate was removed by filteration and washed twice with ice-cold acetone then dried under vacuum.

Yield 58%.

Anal. Calcd (Found, %) $C_{18}H_{36}N_6O_4ClS_2Cr \cdot H_2O$ (Fw. 570.12)

C, 37.92 (37.98) : H, 6.72 (7.03) : N, 14.74 (14.44).

UV/Vis. (in DMF)

λ_{541nm} (ε=134.5 M^{-1} cm^{-1}), λ_{406nm} (ε=77.5 M^{-1} cm^{-1}).

Λ_M (in DMF) : 91.9 ohm^{-1} cm^2 mol^{-1}.

5) *cis*-[Cr([14]-decane)(N_3)$_2$]ClO_4.

cis-[Cr([14]-decane)$(OH)_2]^+$ solution (2 mmol, 10 mL) was acidified with the $HClO_4$ (70%, *ca.* 1 mL). The resulting solution was mixed with the aqueous solution of NaN_3 (0.65 g in 50 mL water). Then saturated $NaClO_4$ solution (4 mL) was added. The resulting mixture was stirred 4 h at room temperature. The product acquired as blue precipitate was removed by filteration and washed twice with ice-cold acetone then dried under vacuum.

Yield 75%.

Anal. Calcd (Found, %) $C_{16}H_{36}N_{10}O_4ClCr$ (Fw. 519.98)

C, 36.96 (36.98): H, 6.98 (6.94): N, 26.94 (26.48).

UV/Vis. (in DMF)

λ_{572nm} (ε=212.5 M^{-1} cm^{-1}), λ_{426nm} (ε=126.5 M^{-1} cm^{-1}).

Λ_M (in DMF) : 73.6 ohm^{-1} cm^2 mol^{-1}.

6) *cis*-[Cr([14]-decane)(ca)$_2$]ClO$_4$

cis-[Cr([14]-decane)(OH)$_2$]$^+$ solution (2 mmol, 10 mL) was acidified with the aqueous solution of chloroacetic acid (1 g in 20 mL water). The mixture was stirred for 1 h. Afterwards, saturated NaClO$_4$ solution (4 mL) was added into the solution and heated at 100℃ with stirring for 2 h. The product acquired as pink precipitate was removed by filteration and washed twice with cold water, then dried under vacuum.

Yield 90%.
Anal. Calcd (Found, %) $C_{20}H_{40}N_4O_8Cl_3Cr$ (Fw. 622.91)
C, 38.56 (38.51); H, 6.47 (6.70); N, 8.99 (9.09).
UV/Vis. (in DMF)
λ_{537nm} (ε=201 M^{-1} cm^{-1}), λ_{390nm} (ε=107.5 M^{-1} cm^{-1}).
Λ_M (in DMF) : 66.2 ohm^{-1} cm^2 mol^{-1}.

7) *cis*-[Cr([14]-decane)(bz)$_2$]ClO$_4$ · 0.5H$_2$O

cis-[Cr([14]-decane)(OH)$_2$]$^+$ solution(10 mmol, 50 mL) was acidified with the methanol solution of benzoic acid (9 g in 20 mL methanol). The saturated NaClO$_4$ solution (20 mL) was added into the mixture solution, and heated at 100℃ for 2 h with stirring.

The pink precipitate was removed by filteration and washed twice with methanol and ether, then dried under vacuum.

Yield 34%.

Anal. Calcd (Found, %) $C_{30}H_{46}N_4O_8ClCr \cdot 0.5H_2O$ (Fw. 687.17)

C, 52.44 (52.65): H, 6.89 (6.96): N, 8.15 (8.22).

UV/Vis. (in DMF)

λ_{550nm} (ε=223 M^{-1} cm^{-1}), λ_{392nm} (ε= 130.5 M^{-1} cm^{-1}).

Λ_M (in DMF) : 67.0 ohm^{-1} cm^2 mol^{-1}.

8) *cis*-[Cr([14]-decane)$(cbz)_2$]ClO_4

cis-[Cr([14]-decane)$(OH)_2$]$^+$ solution (2 mmol, 10 mL) was acidified with the methanol solution of *p*-chlorobenzoic acid (1.6 g in 40 mL methanol). Saturated $NaClO_4$ solution (4 mL) was added to the resulting mixture then heated at 100℃ for 2 h with stirring. The pink precipitate was removed by filteration and washed twice with methanol and ether, then dried under vacuum.

Yield 50%.

Anal. Calcd (Found, %) $C_{30}H_{44}N_4O_8Cl_3Cr$ (Fw. 742.053)

C, 48.23 (48.29): H, 5.94 (6.06): N, 7.50 (7.57).

UV/Vis. (in DMF)

λ_{547nm} (ε=221 M^{-1} cm^{-1}), λ_{394nm} (ε=126.5 M^{-1} cm^{-1}).

Λ_M (in DMF) : 67.1 ohm^{-1} cm^2 mol^{-1}.

9) *cis*-[Cr([14]-decane)(ox)]$ClO_4 \cdot 0.5H_2O$.

cis-[Cr([14]-decane)$(OH)_2]^+$ solution (2 mmol, 10 mL) was acidified with the oxalic acid aqueous solution (2 g in 12 mL water). Saturated $NaClO_4$ solution (4 mL) was added into the solution, and the resulting mixture was stirred at 100℃ for 5 min. The mixture was cooled down to 0℃. The pink precipitate was removed by filteration and washed twice with ice-cold acetone, then dried under vacuum. This crude material was purified by dissolving in about 120 mL of water at 100℃. The product was acquired as precipitate by the slow addition of saturated $NaClO_4$ solution (12 mL), then cooled to 0℃.

Yield 84%.

Anal. Calcd (Found, %) $C_{18}H_{36}N_4O_8ClCr \cdot 0.5H_2O$ (Fw. 532.96)

C, 40.57 (40.60) : H, 7.00 (7.27) : N, 10.51 (10.48).

UV/Vis. (in DMF)

λ_{532nm} (ε=157 M^{-1} cm^{-1}), λ_{385nm} (ε=82 M^{-1} cm^{-1}).

Λ_M (in DMF) : 67.9 ohm^{-1} cm^2 mol^{-1}.

10) *cis*-[Cr([14]-decane)(mal)]$ClO_4 \cdot 0.25H_2O$

cis-[Cr([14]-decane)$(OH)_2]^+$ solution (2 mmol, 10 mL) was acidified with the malonic acid aqueous solution (2 g in 12 mL water). The saturated $NaClO_4$ solution (4 mL) was added into the solution and the resulting mixture was stirred at 100℃ for 5 min. The mixture was cooled down to 0℃. The pink precipitate was removed by filteration and washed twice with ice-cold acetone, then dried under vacuum. This crude material was purified by dissolving in about 200 mL of water at 100℃. The product was acquired as precipitate by slow addition of saturated $NaClO_4$ solution (20 mL), then cooled to 0℃.

Yield 41%.

Anal. Calcd (Found, %) $C_{19}H_{38}N_4O_8ClCr \cdot 0.25H_2O$ (Fw. 542.48)

C, 42.07 (42.09) : H, 7.15 (6.97) : N, 10.33 (10.32).

UV/Vis. (in DMF)

λ_{550nm} (ε=164 M^{-1} cm^{-1}), λ_{387nm} (ε= 70.5 M^{-1} cm^{-1}).

Λ_M (in DMF) : 70.3 ohm^{-1} cm^2 mol^{-1}.

11) *cis*-[Cr([14]-decane)(acac)]$(ClO_4)_2 \cdot 0.5H_2O$

A mixture of *cis*-[Cr([14]-decane)$(OH)_2]^+$ solution (2 mmol, 10 mL) and acetylacetone (2 mL) was stirred overnight at room temperature. The saturated $NaClO_4$ solution (4 mL) was added into the mixture. The resulting mixture stirred vigourously at 100℃ for 5 min then cooled down to 0℃. The pink precipitate was removed by filteration and washed twice with water and ether, then dried under vacuum.

Yield 68%.

Anal. Calcd (Found, %) $C_{21}H_{42}N_4O_{10}Cl_2Cr \cdot 0.5H_2O$ (Fw. 643.50)

C, 39.20 (39.17) : H, 6.89 (7.12) : N, 8.71 (9.03).

UV/Vis. (in DMF)

λ_{536nm} (ε=190 M^{-1} cm^{-1}), λ_{390nm} (ε=296 M^{-1} cm^{-1}),

λ_{354nm} (ε=761 M^{-1} cm^{-1}).

Λ_M (in DMF) : 149 ohm^{-1} cm^2 mol^{-1}.

12) *cis*-$[\{Cr([14]\text{-decane})(\mu\text{-cit})\}_2](ClO_4)_2 \cdot 6H_2O$.

cis-$[Cr([14]\text{-decane})(OH)_2]^+$ solution (2 mmol, 10 mL) was acidified with the aqueous citric acid solution (2 g in 20 mL water). Afterwards, saturated $NaClO_4$ solution (4 mL) was added into the solution. The resulting mixture was heated at 100℃ with stirring for 5 min then cooled to 0℃. The product acquired as pink precipitate was removed by filteration and washed twice with ice-cold water, then dried under vacuum.

Yield 34%.

Anal. Calcd (Found, %) $C_{44}H_{84}N_8O_{22}Cl_2Cr_2 \cdot 6H_2O$ (Fw. 1359.13)

C, 38.85 (38.88): H, 7.11 (6.97): N, 8.24 (8.21).

UV/Vis. (in DMF)

λ_{532nm} (ε=186 M^{-1} cm^{-1}), λ_{385nm} (ε=97 M^{-1} cm^{-1}).

Λ_M (in DMF) : 168.6 ohm^{-1} cm^2 mol^{-1}.

5. X-ray Diffraction Measurements

1) X-ray diffraction of *cis*-[Cr([14]-decane)$(NCS)_2$]$ClO_4 \cdot H_2O$

The single crystal of *cis*-[Cr([14]-decane)$(NCS)_2$]$ClO_4 \cdot H_2O$ suitable for structure determination was acquired from acetonitrile and H_2O (1 : 1 v/v) mixed solvent, by slow evaporation of solvent at room temperature. The essential experimental conditions for the crystal structure determination and resulting crystal data were summarized in Table 1, and atomic coordinates were given in Table 2. The single crystal of *cis*-[Cr([14]-decane)$(NCS)_2$]$ClO_4 \cdot H_2O$ was mounted on a glass fiber and coated with epoxy resin. X-ray data were collected at room temperature using graphite-monochromated Mo K_α radiation on a Kappa CCD diffractometer. Data were corrected for Lorentz and polarization effects. Absorption correction was not made. For *cis*-[Cr([14]-decane)$(NCS)_2$]$ClO_4 \cdot H_2O$, among 6039 reflections measured in the range $1.41 \leq 2\theta \leq 27.45$, 6030 were assumed to be observed ($F > 4\sigma(F)$). The crystal structure was solved by the direct method, and refined by full-matrix least-squares refinement using the SHELXL-97 computer program.[30] All non-hydrogen atoms were refined anisotropically. The positions of all hydrogen atoms were allowed to ride on their bonded atoms with the isotropic displacement factors fixed with values of 1.2 times those of the bonded atoms.

Table 1. Crystallographic Data for *cis*-$[Cr([14]\text{-decane})(NCS)_2]ClO_4 \cdot H_2O$

Formula	$C_{18}H_{38}N_6O_5S_2ClCr$
Formula weight	570.11
Radiation (Å)	Mo Kα (0.71073)
Crystal system	orthorhombic
Space group	P*bca*
a (Å)	15.295
b (Å)	16.4850(10)
c (Å)	21.0490(10)
α (°)	90
β (°)	90
γ (°)	90
V (Å^3)	5307.3(4)
Z	8
T(K)	293(2)
D_{calc} (g cm^{-3})	1.427
μ (mm^{-1})	0.728
no. unique data	6039
no. of obsd data ($F_0\rangle\ 4\sigma(F_0)$)	6030
no. variable	304
Goodness of fit	1.008
R (abs, all)	0.0767, 0.2019
R_w (obs, all)	0.2196, 0.2818

Table 2. Atomic Coordinates ($\times 10^4$) and Equivalent Isotropic Displacement Parameters ($Å^2 \times 10^3$) for *cis*-[Cr([14]-decane)$(NCS)_2]ClO_4 \cdot H_2O$

	x	*y*	*z*	*U* (eq)
Cr(1)	2766(1)	174(1)	3453(1)	37(1)
N(1)	3046(3)	1170(2)	2827(2)	49(1)
N(2)	3425(3)	814(2)	4173(2)	48(1)
N(3)	2367(3)	-613(2)	4202(2)	45(1)
N(4)	1551(3)	759(2)	3549(2)	43(1)
N(5)	3819(3)	-499(3)	3373(2)	49(1)
N(6)	2281(3)	-408(3)	2698(2)	51(1)
C(1)	3914(4)	1595(3)	2818(3)	68(2)
C(2)	4589(4)	1030(4)	2532(3)	73(2)
C(3)	3856(6)	2381(4)	2405(4)	97(3)
C(4)	4168(5)	1838(3)	3493(3)	73(2)
C(5)	4291(3)	1197(3)	4006(3)	56(2)
C(6)	4742(4)	1538(4)	4596(4)	82(2)
C(7)	3513(4)	225(3)	4712(3)	58(2)
C(8)	2660(4)	-201(3)	4813(3)	59(2)
C(9)	1446(4)	-957(3)	4249(3)	61(2)

Table 2. *Continued*

	x	y	z	U (eq)
C(10)	1356(4)	-1596(3)	3738(4)	75(2)
C(11)	1286(5)	-1371(4)	4897(3)	82(2)
C(12)	777(4)	-289(3)	4210(3)	62(2)
C(13)	757(3)	230(3)	3603(3)	51(2)
C(14)	-105(4)	708(4)	3605(4)	80(2)
C(15)	1480(4)	1315(3)	2985(3)	56(2)
C(16)	2315(4)	1754(3)	2899(3)	63(2)
C(17)	4519(4)	-834(4)	3455(3)	55(2)
C(18)	2158(4)	-724(3)	2225(3)	51(2)
S(1)	5442(1)	-1247(1)	3578(1)	77(1)
S(2)	1935(2)	-1166(1)	1550(1)	87(1)
Cl(1)	3327(1)	2093(1)	149(1)	79(1)
O(1)	2523(4)	1762(4)	384(4)	142(3)
O(2)	4036(5)	1561(5)	274(5)	198(4)
O(3)	3182(7)	2081(4)	-499(3)	189(4)
O(4)	3545(4)	2758(3)	496(3)	153(3)
OW1	2848(5)	758(5)	1478(3)	150(3)

U(eq) was defined as one third of the trace of the orthogonalized U_{ij} tensor.

2) X-ray diffraction of *cis*-[Cr([14]-decane)(cbz)$_2$]ClO$_4$

The single crystal of *cis*-[Cr([14]-decane)(cbz)$_2$]ClO$_4$ suitable for structure determination was acquired from acetonitrile and H_2O(1 : 1 v/v) mixed solvent, by slow evaporation of solvent at room temperature. The essential experimental conditions for the crystal structure determination and resulting crystal data were summarized in Table 3, and atomic coordinates were given in Table 4. The single crystal of *cis*-[Cr([14]-decane)(cbz)$_2$]ClO$_4$ was mounted on a glass fiber and coated with epoxy resin. X-ray data were collected at room temperature using graphite-monochromated Mo K_α radiation on a Kappa CCD diffractometer. Data were corrected for Lorentz and polarization effects. Absorption correction was not made. For *cis*-[Cr([14]-decane) (cbz)$_2$]ClO$_4$, among 7999 reflections measured in the range $1.41 \leq 2\theta \leq 27.45$, 7913 were assumed to be observed ($F > 4\sigma(F)$). The crystal structures were solved by the direct method, and refined by full-matrix least-squares refinement using the SHELXL-97 computer program.[30] All non-hydrogen atoms were refined anisotropically. The positions of all hydrogen atoms were allowed to ride on their bonded atoms with the isotropic displacement factors fixed with values of 1.2 times those of the bonded atoms.

Table 3. Crystallographic Data for *cis*-[Cr([14]-decane)(cbz)$_2$]-ClO_4

Formula	$C_{30}H_{44}N_4O_8Cl_3Cr$
Formula weight	747.04
Radiation (Å)	Mo K_α(0.71073)
Crystal system	orthorhombic
Space group	P*bca*
a (Å)	12.0930(10)
b (Å)	20.3580(10)
c (Å)	28.852
α (°)	90
β (°)	90
γ (°)	90
V (Å^3)	7103.1(7)
Z	8
T(K)	293(2)
D_{calc} (g cm^{-3})	1.397
μ (mm^{-1})	0.600
no. unique data	7999
no. of obsd data ($F_0 > 4\sigma(F_0)$)	7913
no. variable	422
Goodness of fit	1.127
R (abs, all)	0.0977, 0.2172
R_w (obs, all)	0.1620, 0.3278

Table 4. Atomic Coordinates ($\times 10^4$) and Equivalent Isotropic Displacement Parameters (Å^2 × 10^3) for *cis*-[Cr([14]-decane)(cbz)$_2$]ClO$_4$

	x	*y*	*z*	*U* (eq)
Cr(1)	741(1)	1562(1)	1199(1)	46(1)
N(1)	1348(4)	825(2)	749(2)	51(1)
N(2)	2407(4)	1906(2)	1257(2)	51(1)
N(3)	604(4)	2334(2)	710(2)	52(1)
N(4)	-821(4)	1216(2)	959(2)	50(1)
C(1)	2395(5)	477(3)	885(2)	56(2)
C(2)	2678(6)	-98(4)	553(3)	81(2)
C(3)	3366(5)	949(3)	904(2)	57(2)
C(4)	3393(5)	1455(3)	1296(2)	53(2)
C(5)	4490(5)	1837(4)	1263(2)	71(2)
C(6)	3359(5)	1130(4)	1770(2)	70(2)
C(7)	2559(5)	2424(3)	892(2)	63(2)
C(8)	1507(5)	2798(3)	827(2)	62(2)
C(9)	-493(5)	2684(3)	672(2)	56(2)
C(10)	-438(7)	3256(4)	329(2)	79(2)
C(11)	-1387(5)	2207(3)	511(2)	64(2)
C(12)	-1774(5)	1669(3)	843(2)	56(2)
C(13)	-2206(5)	1946(4)	1305(2)	73(2)
C(14)	-2736(5)	1297(4)	614(2)	76(2)
C(15)	-606(5)	735(3)	588(2)	64(2)
C(16)	424(5)	355(3)	685(2)	61(2)
C(17)	10(6)	593(3)	1915(2)	60(2)

Table 4. *Continued*

	x	y	z	U (eq)
C(18)	297(5)	307(3)	2375(2)	50(2)
C(19)	−405(5)	−154(3)	2566(2)	61(2)
C(20)	−188(7)	−430(3)	2995(3)	71(2)
C(21)	750(7)	−235(4)	3227(2)	71(2)
C(22)	1450(6)	227(4)	3049(3)	78(2)
C(23)	1227(5)	492(4)	2616(2)	64(2)
C(24)	679(6)	2412(3)	2028(2)	59(2)
C(25)	10(5)	2821(3)	2353(2)	53(2)
C(26)	456(6)	2987(3)	2776(2)	60(2)
C(27)	−115(7)	3383(4)	3085(2)	72(2)
C(28)	−1150(6)	3591(3)	2967(3)	67(2)
C(29)	−1617(6)	3439(4)	2547(3)	78(2)
C(30)	−1021(6)	3051(4)	2239(3)	71(2)
O(1)	787(3)	907(2)	1699(1)	51(1)
O(2)	−931(4)	516(3)	1761(2)	104(2)
O(3)	216(3)	2220(2)	1650(1)	55(1)
O(4)	1649(4)	2284(3)	2131(2)	87(2)
Cl(1)	1018(2)	−574(1)	3770(1)	125(1)
Cl(2)	−1898(2)	4071(1)	3360(1)	103(1)
Cl(3)	−3994(2)	1459(1)	−4464(1)	72(1)
O(5)	1294(8)	1899(5)	−199(3)	215(5)
O(6)	−5139(6)	1399(5)	−4411(3)	170(3)
O(7)	−3669(9)	861(4)	−4652(3)	193(4)
O(8)	−3416(6)	1578(3)	−4052(2)	118(2)

U(eq) was defined as one third of the trace of the orthogonalized U_{ij} tensor.

3) X-ray diffraction of *cis*-[Cr([14]-decane)(acac)]$(ClO_4)_2 \cdot 0.5H_2O$

The single crystal of *cis*-[Cr([14]-decane)(acac)]$(ClO_4)_2 \cdot 0.5H_2O$ suitable for structure determination was acquired from acetonitrile and H_2O (1 : 1 v/v) mixed solvent, by slow evaporation of solvent at room temperature. The essential experimental conditions for the crystal structure determination and crystal data were summarized in Table 5. The atomic coordinates were given in Table 6. The single crystal of *cis*-[Cr([14]-decane)(acac)]$(ClO_4)_2 \cdot 0.5H_2O$ was mounted on a glass fiber and coated with epoxy resin. X-ray data were collected at room temperature using graphite-monochromated Mo K_α radiation on a Kappa CCD diffractometer. Data were corrected for Lorentz and polarization effects. Absorption correction was not made. For *cis*-[Cr([14]-decane)-(acac)]$(ClO_4)_2 \cdot 0.5H_2O$, among 6975 reflections measured in the range $1.35 \le 2\theta \le 27.48$, 6905 were assumed to be observed ($F > 4\sigma(F)$). The crystal structure was solved by the direct method, and refined by full-matrix least-squares refinement using the SHELXL-97 computer program.[30] All non-hydrogen atoms were refined anisotropically. The positions of all hydrogen atoms were allowed to ride on their bonded atoms with the isotropic displacement factors fixed with values of 1.2 times those of the bonded atoms.

Table 5. Crystallographic Data for *cis*-[Cr([14]-decane)(acac)]$(ClO_4)_2 \cdot 0.5H_2O$

Formula	$C_{21}H_{43}N_4O_{11}Cl_2Cr$
Formula weight	650.49
Radiation(Å)	Mo Kα(0.71073)
Crystal system	monoclinic
Space group	C2/*c*
a (Å)	20.0210(10)
b (Å)	30.1120(10)
c (Å)	12.708
α (°)	90
β (°)	127.2170(10)
γ (°)	90
V (Å^3)	6101.1(4)
Z	8
T (K)	293(2)
D_{calc} (g cm^{-3})	1.416
μ (mm^{-1})	0.608
no. unique data	6975
no. of obsd data ($F_0 > 4\sigma(F_0)$)	6905
no. variable	362
Goodness of fit	1.105
R (abs, all)	0.0824, 0.1143,
R_w (obs, all)	0.2179, 0.2893

Table 6. Atomic Coordinates ($\times 10^4$) and Equivalent Isotropic Displacement Parameters ($Å^2 \times 10^3$) for *cis*-[Cr([14]-decane)-(acac)]$(ClO_4)_2 \cdot 0.5H_2O$

	x	*y*	*z*	*U* (eq)
Cr(1)	2383(1)	1217(1)	1888(1)	37(1)
N(1)	1692(2)	1816(1)	1431(3)	44(1)
N(2)	3232(2)	1432(1)	3867(3)	49(1)
N(3)	3063(2)	609(1)	2640(3)	46(1)
N(4)	1459(2)	940(1)	1993(3)	44(1)
C(1)	2107(3)	2261(1)	2031(4)	52(1)
C(2)	2512(3)	2409(2)	1381(5)	64(1)
C(3)	1463(4)	2613(2)	1727(6)	72(1)
C(4)	2752(3)	2220(2)	3533(4)	63(1)
C(5)	3504(3)	1912(2)	4094(4)	61(1)
C(6)	4169(4)	2007(2)	5572(6)	93(2)
C(7)	3952(3)	1124(2)	4461(4)	63(1)
C(8)	3640(3)	660(2)	4110(4)	64(1)
C(9)	2636(3)	158(1)	2198(4)	52(1)
C(10)	3253(4)	-216(2)	3041(6)	72(1)
C(11)	2303(3)	82(2)	771(5)	61(1)
C(12)	1927(3)	146(2)	2337(5)	59(1)
C(13)	1193(3)	469(1)	1538(4)	52(1)
C(14)	487(3)	327(2)	1607(6)	77(2)

Table 6. *Continued*

	x	y	z	U (eq)
C(15)	724(3)	1249(1)	1192(5)	55(1)
C(16)	1022(3)	1719(2)	1587(5)	56(1)
C(17)	3975(3)	1515(2)	806(5)	69(1)
C(18)	3184(2)	1386(1)	623(4)	45(1)
C(19)	2488(3)	1253(2)	-606(4)	53(1)
C(20)	1740(2)	1111(1)	-865(3)	44(1)
C(21)	1022(3)	985(2)	-2236(4)	60(1)
O(1)	1617(2)	1073(1)	8(2)	43(1)
O(2)	3221(2)	1409(1)	1666(2)	47(1)
Cl(1)	1831(1)	1304(1)	-4710(1)	70(1)
O(3)	2310(4)	1098(2)	-5095(6)	122(2)
O(4)	1393(6)	975(3)	-4593(12)	200(4)
O(5)	2352(9)	1361(5)	-3391(8)	255(6)
O(6)	1437(9)	1693(3)	-5298(11)	220(5)
Cl(2)	5000(0)	282(1)	2500	75(1)
O(7)	4677(7)	533(3)	2941(16)	256(6)
O(8)	4453(14)	67(9)	1752(16)	586(26)
Cl(3)	0	2206(1)	7500	93(1)
O(9)	637(5)	1965(2)	8491(5)	174(3)
O(10)	289(5)	2529(3)	7018(11)	193(4)
O(1W)	4341(12)	1033(6)	-2620(16)	328(8)

U(eq) was defined as one third of the trace of the orthogonalized U_{ij} tensor.

4) X-ray diffraction of *cis*-$[\{Cr([14]\text{-decane})(\mu\text{-cit})\}_2](ClO_4)_2 \cdot 6H_2O$

The single crystal of *cis*-$[\{Cr([14]\text{-decane})(\mu\text{-cit})\}_2](ClO_4)_2 \cdot 6H_2O$ suitable for structure determination was acqured from acetonitrile and H_2O(1 : 1 v/v) mixture solvent, by slow evaporation of solvent at room temperature. The essential experimental conditions for the crystal structure determination and resulting crystal data were summarized in Table 7, and atomic coordinates were given in Table 8. The single crystal of *cis*-$[\{Cr([14]\text{-decane})(\mu\text{-cit})\}_2](ClO_4)_2 \cdot 6H_2O$ was mounted on a glass fiber and coated with epoxy resin. X-ray data were collected at room temperature using graphite-monochromated Mo K_α radiation on a Kappa CCD diffractometer. Data were corrected for Lorentz and polarization effects. Absorption correction was not made. For *cis*-$[\{Cr([14]\text{-decane})(\mu\text{-cit})\}_2](ClO_4)_2 \cdot 6H_2O$, among 2897 reflections measured in the range $1.35 \leq 2\theta \leq 27.48$, 2891 were assumed to be observed ($F > 4\sigma(F)$). The crystal structure was solved by the direct method, and refined by full-matrix least-squares refinement using the SHELXL-97 computer program.[30] All non-hydrogen atoms were refined anisotropically. The positions of all hydrogen atoms were allowed to ride on their bonded atoms with the isotropic displacement factors fixed with values of 1.2 times those of the bonded atoms.

Table 7. Crystallographic Data for *cis*-[{Cr([14]-decane)(μ-cit)}$_2$] -(ClO$_4$)$_2$ · 6H$_2$O

Formula	$C_{22}H_{46}N_4O_{14}ClCr$
Formula weight	678.08
Radiation(Å)	Mo Kα (0.71073)
Crystal system	monoclinic
Space group	C2/*c*
a (Å)	23.818(2)
b (Å)	21.139(2)
c (Å)	16.1350(10)
α (°)	90
β (°)	127.294(4)
γ (°)	90
V (Å^3)	6462.8(9)
Z	8
T(K)	293(2)
D_{calc} (g cm^{-3})	1.394
μ (mm^{-1})	0.504
no. unique data	2897
no. of obsd data ($F_0 > 4\sigma(F_0)$)	2891
no. variable	388
Goodness of fit	1.074
R (abs, all)	0.0865, 0.1486
R_w (obs, all)	0.2574, 0.3303

Table 8. Atomic Coordinates ($\times 10^4$) and Equivalent Isotropic Displacement Parameters ($\text{Å}^2 \times 10^3$) for *cis*-$[\{\mathrm{Cr([14]\text{-}decane)(\mu\text{-}cit)}\}_2](\mathrm{ClO_4})_2 \cdot 6\mathrm{H_2O}$

	x	*y*	*z*	*U* (eq)
Cr(1)	2176(1)	1726(1)	1717(1)	52(1)
N(1)	2152(5)	810(4)	2209(7)	61(3)
N(2)	1104(5)	1579(5)	371(7)	65(3)
N(3)	1709(5)	2214(5)	2301(6)	61(3)
N(4)	3139(5)	1802(4)	3235(6)	60(3)
C(1)	1848(7)	280(6)	1390(10)	73(4)
C(2)	1937(9)	-366(6)	1854(11)	102(5)
C(3)	1061(8)	400(6)	524(10)	81(4)
C(4)	839(7)	944(6)	-240(10)	75(4)
C(5)	48(8)	936(8)	-1036(11)	108(5)
C(6)	1160(7)	900(6)	-821(9)	74(4)
C(7)	671(7)	1803(7)	695(10)	78(4)
C(8)	979(6)	2385(7)	1360(9)	80(4)
C(9)	2078(6)	2799(6)	2946(9)	68(4)
C(10)	1634(7)	3155(7)	3210(10)	81(4)
C(11)	2789(7)	2621(7)	3934(9)	77(4)
C(12)	3378(7)	2400(6)	3872(9)	64(3)
C(13)	3558(7)	2881(6)	3384(10)	80(4)
C(14)	4047(7)	2270(7)	5009(9)	88(4)
C(15)	3211(7)	1225(6)	3835(8)	75(4)

Table 8. *Continued*

	x	*y*	*z*	*U* (eq)
C(16)	2899(6)	664(6)	3104(8)	70(4)
C(17)	3278(9)	1371(5)	1441(9)	57(3)
C(18)	1929(8)	2803(7)	309(12)	71(4)
C(19)	2100(7)	3498(6)	355(9)	68(4)
C(20)	1636(7)	3872(6)	-626(9)	61(3)
C(21)	1828(8)	4560(7)	-388(9)	76(4)
C(22)	1338(10)	5032(9)	-1239(13)	100(5)
Cl(1)	1374(3)	953(2)	3778(3)	101(2)
O(1)	2649(5)	1344(3)	1172(6)	55(2)
O(2)	3814(5)	1546(4)	2293(7)	76(3)
O(3)	2216(4)	2553(4)	1231(6)	63(2)
O(4)	1556(6)	2510(4)	-514(7)	95(3)
O(5)	926(5)	3811(5)	-1012(7)	87(3)
O(6)	1295(7)	4958(6)	-2059(9)	121(4)
O(7)	1041(7)	5437(6)	-1110(9)	120(4)
O(8)	931(9)	891(8)	4055(13)	191(7)
O(9)	1417(11)	1597(6)	3635(12)	191(8)
O(10)	2007(10)	710(10)	4688(17)	250(10)
O(11)	1202(11)	591(7)	2970(13)	187(7)
OW1	0	2305(13)	2500	202(10)
OW2	0	3702(16)	2500	263(15)
OW3	-27(12)	4159(18)	5533(16)	358(20)
OW4	266(9)	4351(11)	1324(14)	239(10)

U(eq) was defined as one third of the trace of the orthogonalized U_{ij} tensor.

III. Results and Discussion

1. Properties of the Spectrum *cis*-$[Cr([14]\text{-decane})(OH)_2]^+$ Solution

The structure of *cis*-$[Cr([14]\text{-decane})(OH)_2]^+$ cation[29] was shown in Fig. 1. The aqueous solution of the compound behaves as a divalent base. From the acid dissociation constants (Table 9)[29] it is known that the *cis*-$[Cr([14]\text{-decane})(OH_2)_2]^{3+}$ cation is a stronger acid than a number of other *cis*-tetraaminediaquachromium(III) cation.

Table 9. Acid Dissociation Constants for Some *cis*-Tetraamine-diaquachromium(III) Complexes at 298K in 1.0 M $NaClO_4$ Solution.

Complexes	pK_1	pK_2
cis-$[Cr(NH_3)_4(OH_2)_2]^{3+}$	4.96	7.53
cis-$[Cr(en)_2(OH_2)_2]^{3+}$	4.75	7.35
cis-$[Cr(trien)(OH_2)_2]^{3+}$	4.47	7.14
cis-$[Cr(cyclam)(OH_2)_2]^{3+}$	4.21	7.25
cis-$[Cr([14]\text{-decane})(OH_2)_2]^{3+}$	3.33	7.02

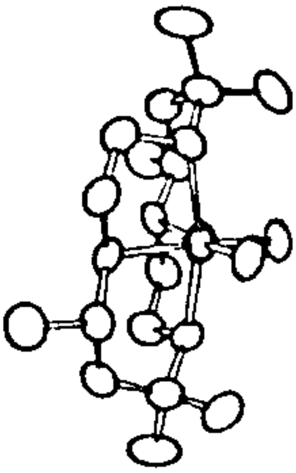

Fig. 1. Configuration of the *cis*-[Cr([14]-decane)$(OH)_2$]$^+$ cation.[29]

All specta are characterized by an increased intensity and a red-shift of a absorption bands compared to other *cis*-tetraamine-diaquachromium(III) complexes.[29] As shown in Fig. 1 a pronounced octahedral distortion of the CrN_4O_2 apparently induced by two methyl groups above and below the CrN_2O_2 plane. Visible absorption spectra of *cis*-[Cr([14]-decane)$(OH)_2$]$^+$ solution were measured by controlling pH with $HClO_4$. The spectral characteristics of *cis*-[Cr([14]-decane)$(OH)_2$]$^+$, *cis*-[Cr([14]-decane)(OH)(H_2O)]$^{2+}$ and *cis*-[Cr([14]-decane)$(OH_2)_2$]$^{3+}$ were illustrated in Fig. 2.

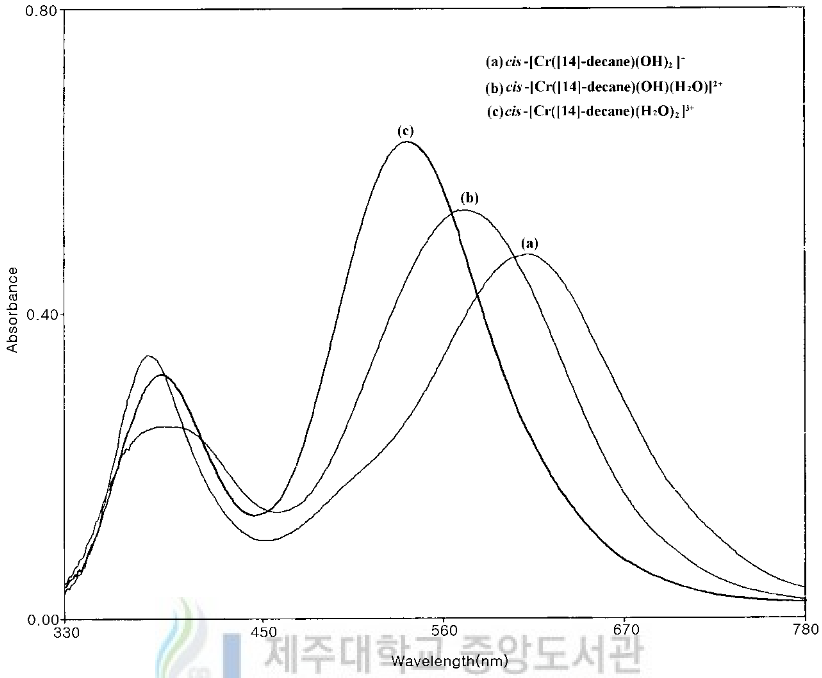

Fig. 2. Visible absorption spectra of *cis*-$[Cr([14]-decane)(OH)_2]^+$ complex and its protonated species.

2. Absorption Spectroscopy

The visible absorption spectra of *cis*-Cr([14]-decane)$(L_a)_m]^{n+}$ (L_a : NCS^-, N_3^-, chloroacetate, benzoate, *p*-chlorobenzoate, oxalate, malonate, acetylacetonate, citrate) in DMF solution at room temperature were represented in Fig. 3~11 and summarized Table 10. As shown Fig. 3~11 and Table 10 the spectra exhibited two bands, at 17400~18800 cm^{-1}(ν_1) and 23400~25900 cm^{-1}(ν_2), due to the $^4A_{2g} \rightarrow {}^4T_{2g}$ and $^4A_{2g} \rightarrow {}^4T_{1g}$ (O_h) transitions, respectively. The assignment of geometric configuration is suggested by inspection of the *d*-*d* absorption spectra. The position and the number of the spin-allowed transitions in the electronic spectra, and their molar absorption coefficients are usually reliable indicators for distinguishing the *cis* and *trans* isomers. In general, the less symmetrical *cis* chromium(III) complexes have two bands in the visible region, and these bands are at higher energies and have higher extinction coefficients than those of more symmetrical *trans*-isomers.[31] As shown in Table 11, the more symmetrical *trans*-isomers of $[CrN_4Cl_2]^+$ chromophores normally have extinction coefficients of <30 and the lowest energy *d*-*d* band ($^4A_{2g} \rightarrow {}^4T_{2g}$) occurs in the range of 16600~17500 cm^{-1}. The less symmetrical *cis*-isomers have much higher extinction coefficients (*ca.* 70~120

M^{-1}cm^{-1}) and lowest energy *d*-*d* band occurred in the region of 18900~20700 cm^{-1}. In these complexes, the nearly symmetric profiles of two quartet bands and the higher extinction coefficient of 134~223 M^{-1} cm^{-1} were evidences of the *cis* configuration. A chromium complexes in tetragonal symmetry are expected to have four absorption bands in *d*-*d* region, but each spectrum apparently has two major components. For the splitting of the two bands, we have fitted the band profiles to four or five Gaussian curves, as shown in Fig. 3~11. The contribution from outside bands was corrected for fine deconvolution. The four peak positions can be assigned to the ^4E ($^4T_{2g}$ in O_h symmetry), $^4B_2$ ($^4T_{2g}$), ^4E ($^4T_{1g}$) and $^4A_2$ ($^4T_{1g}$), respectively, as shown in Table 12.[36, 37]

Table 10. Electronic Transition Spectral Data of *cis*-Cr([14]-decane)($(L_a)_m]^{n+}$ Complexes at 298K in DMF

L_a	spin-allowed transition		ε_1 (M^{-1} cm^{-1})	ε_2 (M^{-1} cm^{-1})	$\varepsilon_1 / \varepsilon_2$
	${}^4A_{2g}\rightarrow{}^4T_{2g}$ (ν_1, cm^{-1})	${}^4A_{2g}\rightarrow{}^4T_{1g}$ (ν_2, cm^{-1})			
NCS^-	18466	24764	134.5	77.5	1.74
N_3^-	17463	23476	212.5	126.5	1.68
ca	18580	25651	201	107.5	1.87
bz	18236	25394	223	130.5	1.71
cbz	18265	25394	221	126.5	1.75
ox	18751	25909	157	82	1.91
mal	18149	25840	164	70.5	2.33
acac	18665	25766	190	269	0.71
cit	18466	25651	186	97	1.92

Table 11. Electronic Transition Spectral Data of *cis*- and *trans*-$[CrN_4L_{a2}]^{n+}$ Chromophores

Complexes	ν_{max} (ε) cm^{-1} (M^{1} cm^{-1})	Ref.
trans-$[Cr(en)_2Cl_2]^+$	17301 (24.5), 22075 (23), 25253 (34)	35
trans-$[Cr(cyclam)Cl_2]^+$	17483 (19.9), 24570 (35), 27397 (41)	34
trans-[Cr(*meso*-[14]-decane)$Cl_2]^+$	17422 (25), 22727 (27), 25840 (47)	31
trans-[Cr(*meso*-[14]-decane)$Br_2]^+$	16667 (33), 24390 (38), 26178 (43)	31
cis-$[Cr(en)_2Cl_2]^+$	18939 (71), 24876 (69)	35
cis-$[Cr(cyclam)Cl_2]^+$	18904 (111), 24752 (106)	34
cis-$[Cr(en)_2(H_2O)_2Cl_2]^{3+}$	20661 (67), 27322 (43)	36
cis-$[Cr(cyclam)(en)_2]^+$	20704 (126), 27027 (38)	34
cis-[Cr(*rac*-[14]-decane)$(NO_3)_2]^+$	19084 (202), 25641 (116)	31

Table 12. Resolved Electronic Absorption Spectral Data of *cis*-Cr([14]-decane)(L_a)$_m$]$^{n+}$ Complexes.

L_a	Noncubic split levels	
	$^4A_{2g} \rightarrow {}^4T_{2g}$ (^4E, $^4B_2$)	$^4A_{2g} \rightarrow {}^4T_{1g}$ (^4E, $^4A_2$)
NCS^-	17325, 19122	24151, 25189
N_3^-	16862, 18241	23432, 24428
ca	17967, 19058	24724, 25814
bz	17364, 18562	24848, 25438
cbz	17644, 18853	25052, 25524
ox	18158, 19672	24205, 26481
mal	17460, 18839	25012, 26290
acac	18032, 19438	25444, 26477
cit	17989, 18690	25140, 25967

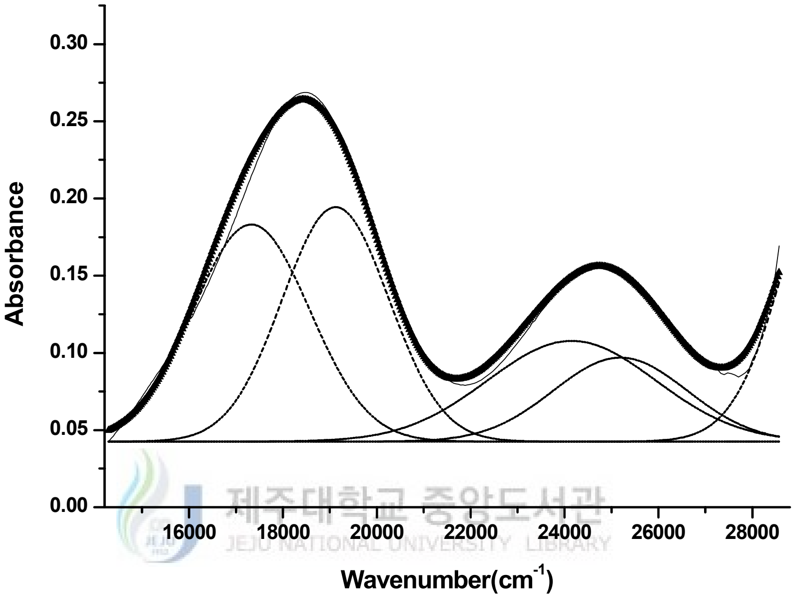

Fig. 3. Electronic absorption spectrum of *cis*-[Cr([14]-decane)(NCS)$_2$]-(ClO$_4$)$_2$ · H$_2$O at 298K in DMF solution.

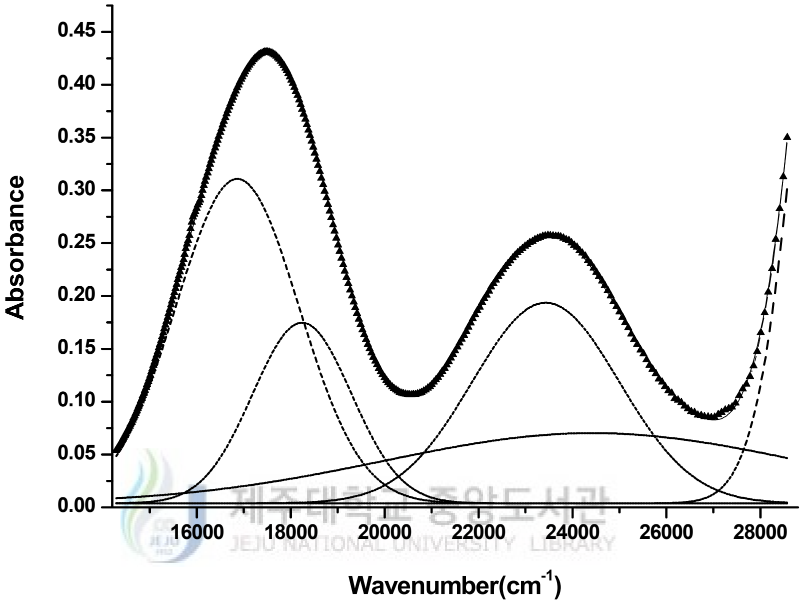

Fig. 4. Electronic absorption spectrum of *cis*-[Cr([14]-decane)$(N_3)_2$]-$(ClO_4)_2$ at 298K in DMF solution.

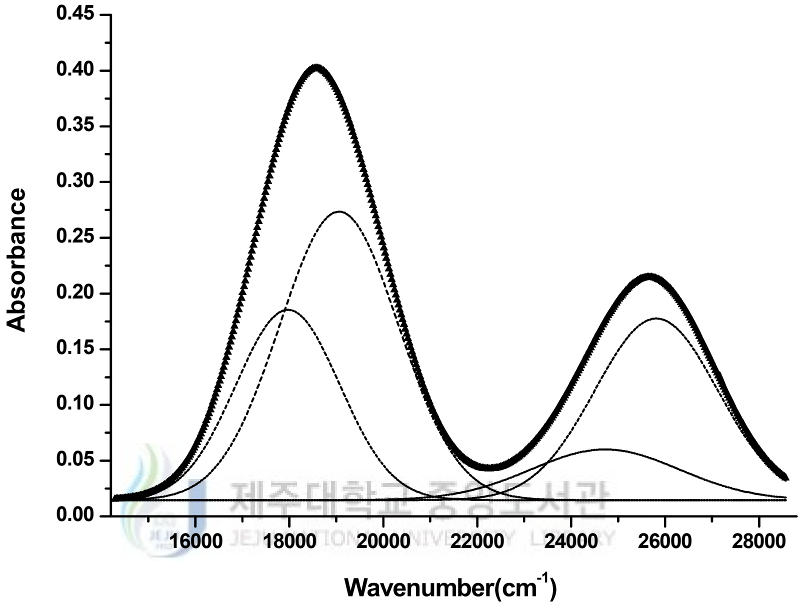

Fig. 5. Electronic absorption spectrum of *cis*-[Cr([14]-decane)(ca)$_2$]-ClO$_4$ at 298K in DMF solution.

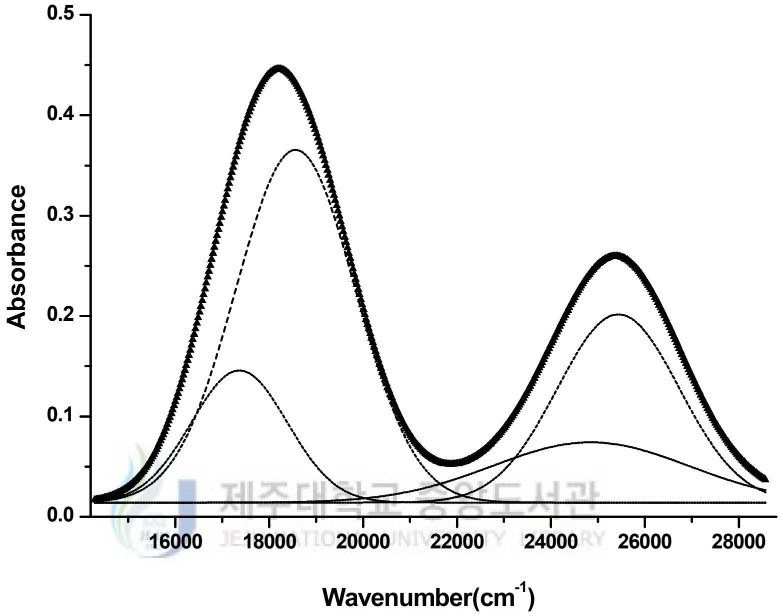

Fig. 6. Electronic absorption spectrum of *cis*-[Cr([14]-decane)(bz)$_2$]-$ClO_4 \cdot 0.5H_2O$ at 298K in DMF solution.

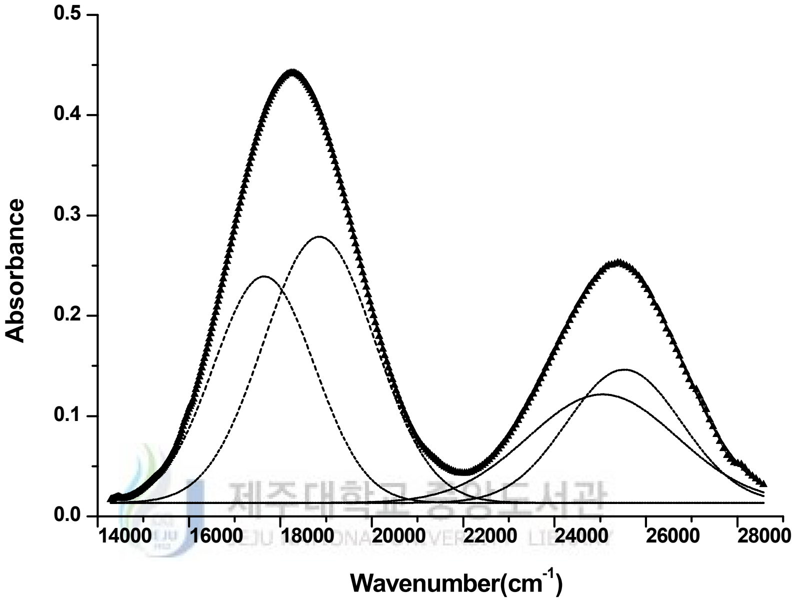

Fig. 7. Electronic absorption spectrum of *cis*-[Cr([14]-decane)(cbz)$_2$]-ClO$_4$ at 298K in DMF solution.

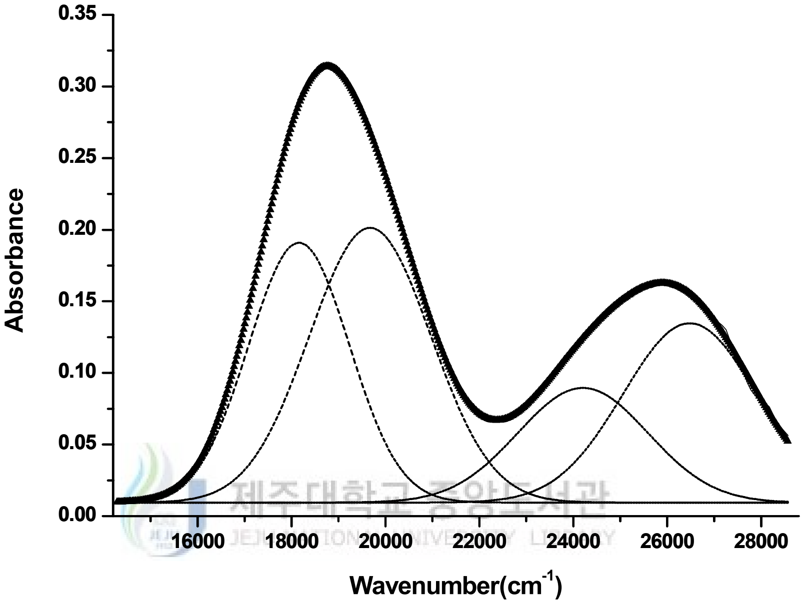

Fig. 8. Electronic absorption spectrum of *cis*-[Cr([14]-decane)(ox)]-$ClO_4 \cdot 0.5H_2O$ at 298K in DMF solution.

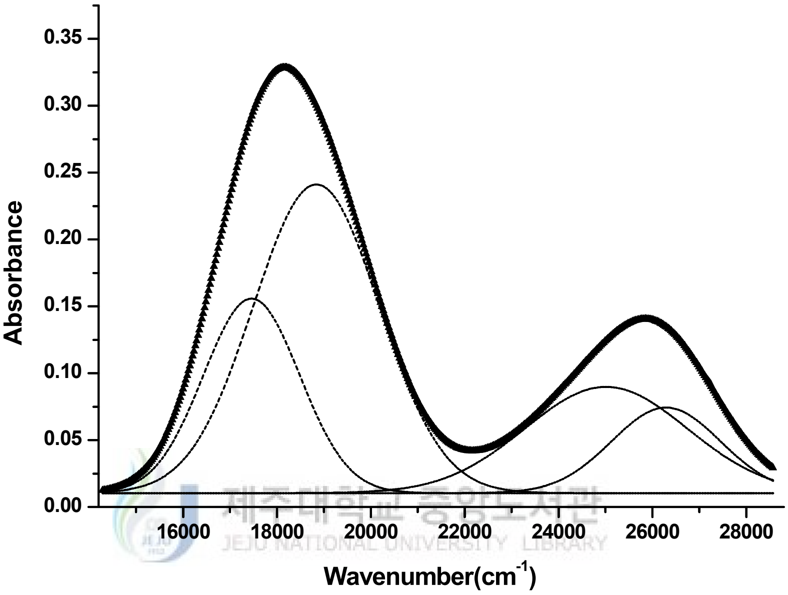

Fig. 9. Electronic absorption spectrum of *cis*-[Cr([14]-decane)(mal)]-$ClO_4 \cdot 0.25H_2O$ at 298K in DMF solution.

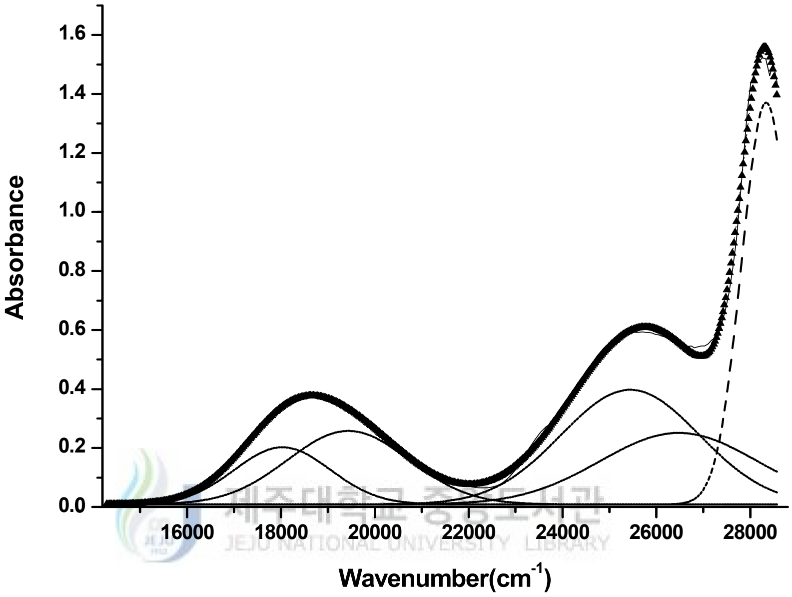

Fig. 10. Electronic absorption spectrum of *cis*-[Cr([14]-decane)(acac)]-$ClO_4 \cdot 0.5H_2O$ at 298K in DMF solution.

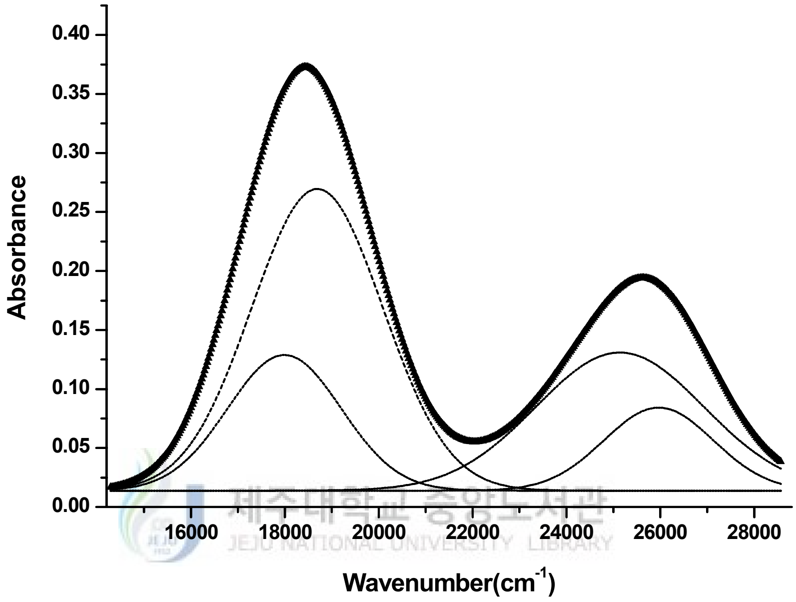

Fig. 11. Electronic absorption spectrum of *cis*-[{Cr([14]-decane)(μ-cit)}$_2$](ClO$_4$)$_2$ · 6H$_2$O at 298K in DMF solution.

3. Infrared Spectroscopy

The mid-infrared spectra of the nine complexes recorded at room temperature were presented in Fig. 12 ~ 20, and summarized at Table 13. The broadness of absorption bands near 3400 cm^{-1} indicated that there were hydrogen bonds in these complexes. Two strong bands in the region of 3300 ~ 3050 cm^{-1} were due to the symmetric and antisymmetric N-H stretching modes. Two strong bands in the region of 2990 ~ 2860 cm^{-1} were due to the symmetric and antisymmetric C-H stretching modes. The N-H wagging mode appeared at near 1250 cm^{-1} as a medium band. The very strong absorption at near 1100 cm^{-1} and near 620 cm^{-1} were assigned to ionic perchlorate.[37] Two peaks at near 440 and near 480 cm^{-1} were assigned to the Cr-N stretching mode.[38, 39] Frequently, the infrared spectroscopy is useful in elucidating structures and determining the number of functional groups involved in coordination. It is well known that *cis* isomer of cyclam chromium(III) complexes exhibits at least three bands in the 900 ~ 830 cm^{-1} region due to the N-H rocking modes, while the methylene vibrational modes exhibit two peaks in the 830 ~770 cm^{-1} region. However, *trans* isomer shows two groups of bands; a doublet near 890 cm^{-1} arises from the secondary amine vibration and only one band near 810 cm^{-1} is mainly due to the methylene vibration.[40] The present complexes exhibited three N-H wagging bands at near 890, near 860 and near 840 cm^{-1} region. Two CH_2 rocking bands were exhibited at near 820 and near 780 cm^{-1}. Since the infrared spectra of the title complexes were consistent with the *cis* configuration.

The IR spectra of the *cis*-$[Cr([14]\text{-decane})(NCS)_2]ClO_4$ complex revealed that the ambidentate thiocyanate ligand was N-bonded[41, 42] (the ν (C-S) vibration occurred 818 cm^{-1} and the strong ν (N-C) vibration occurred 2073 cm^{-1}). In general, the transition metal complexes containing a terminal azide ligand exhibit an intense antisymmetric friquency, ν_{as} (N_3) at near 2090 cm^{-1} and a symmetric mode, $\nu_s(N_3)$ at $\sim$1350 cm^{-1} and deformation band at near 620 cm^{-1}.[43] The IR spectra of the *cis*-$[Cr([14]\text{-decane})(N_3)_2]$-$ClO_4$ complex at 2081 cm^{-1} were assigned as the antisymmetric stretching mode of azide. The ν_s (N_3) stretching frequency and δ (N_3) deformation band were observed at 1344 and 636 cm^{-1} respectively.

Two stretching frequencies ν_{as} (COO^-) and ν_s (COO^-) found at near 1600 and near 1350 cm^{-1} revealed that the carboxylate oxygen was coordinated.[37] Unidentate carboxylate complexes have much greater $\Delta\nu$ [between $\nu_{as}(COO^-)$ and $\nu_s(COO^-)$] values than the ionic compounds. Since there were large $\Delta\nu$ values (oxalate: 296 cm^{-1}, malonate: 296 cm^{-1}, bezonate: 242 cm^{-1}, p-chlorobezonate: 257 cm^{-1}, chloroacetate : 338 cm^{-1}, citratate: 230 cm^{-1}), carboxylates coordinated as unidentate.[37] The carbonyl vibration ν_{as} (C=O) of acetylacetonate splitted into two peaks and exhibited in the 1610 ~ 1535 cm^{-1} region.

X-ray crystal analyses also performed to establish the details of those coordination and to verify these geometric assignment.

Table 13. IR Spectral Data (cm^{-1}) of the *cis*-[Cr([14]-decane)$(L_a)_m$]$(ClO_4)_n \cdot xH_2O$ Complexes

L_a	macrocycle (-NH)					
	asymmetric	symmetric	wagging	rocking		
NCS^-	3204	3051	1271	891	860	844
N_3^-	3220	3052	1271	889	860	842
ca	3225	3094	1234	894	864	
bz	3205	3065	1246	903	864	
cbz	3205	3070	1244	892	863	849
ox	3211	3136	1240	889	860	829
mal	3224	3082	1274	896	863	
acac	3209	3076	1284	904	864	
cit	3216	3109	1273	894	864	835

Table 13. *Continued*

L_a	macrocycle-CH)			
	asymmetric	symmetric	rocking	
NCS^-	2978	2887	817	777
N_3^-	2980	2889	819	777
ca	2983	2881	819	786
bz	2971	2877	825	779
cbz	2974	2870	830	771
ox	2968	2895	808	792
mal	2975	2891	818	779
acac	2976	2918	820	776
cit	2977	2891	819	779

Table 13. *Continued*

L_a	Cr–N		ionic perchlorate		coordinate ligand
NCS^-	482	437	1109	625	2073, 818
N_3^-	482	435	1109	625	2081, 1344, 636
ca	484	439	1107	625	1684, 1346
bz	469	440	1120	623	1609, 1367
cbz	474	431	1098	625	1609, 1352
ox	474	403	1102	623	1678, 1382
mal	461		1101	626	1656, 1360
acac	468	431	1110	628	1610, 1356
cit	484	439	1104	626	1731, 1620, 1390

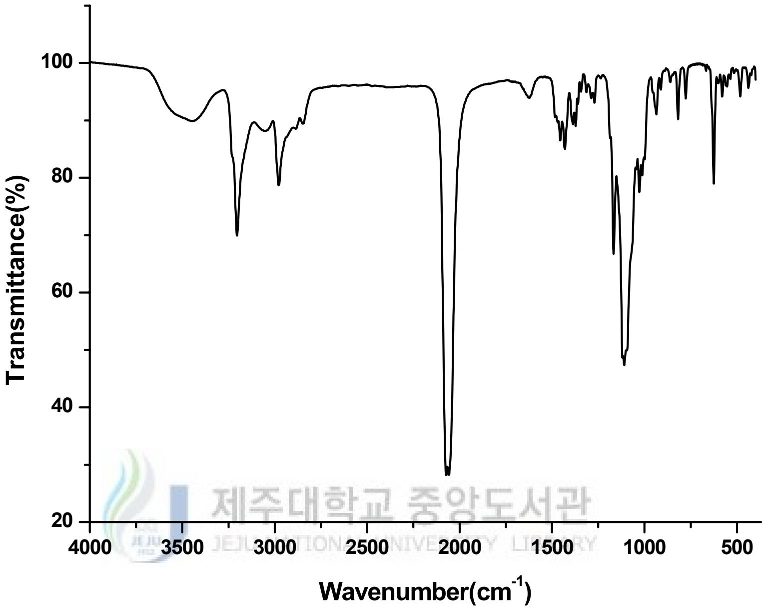

Fig. 12. IR spectrum of *cis*-[Cr([14]-decane)(NCS)$_2$]ClO$_4$ · H$_2$O.

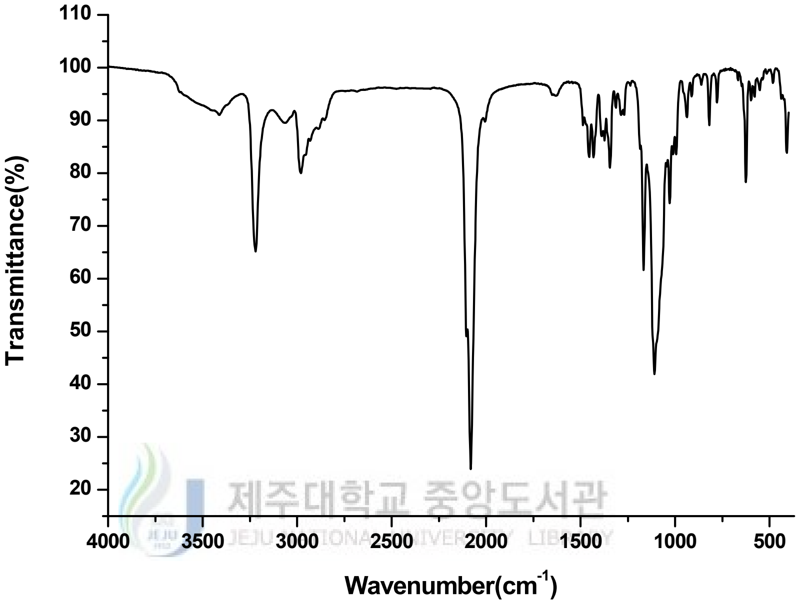

Fig. 13. IR spectrum of *cis*-[Cr([14]-decane)$(N_3)_2$]ClO_4.

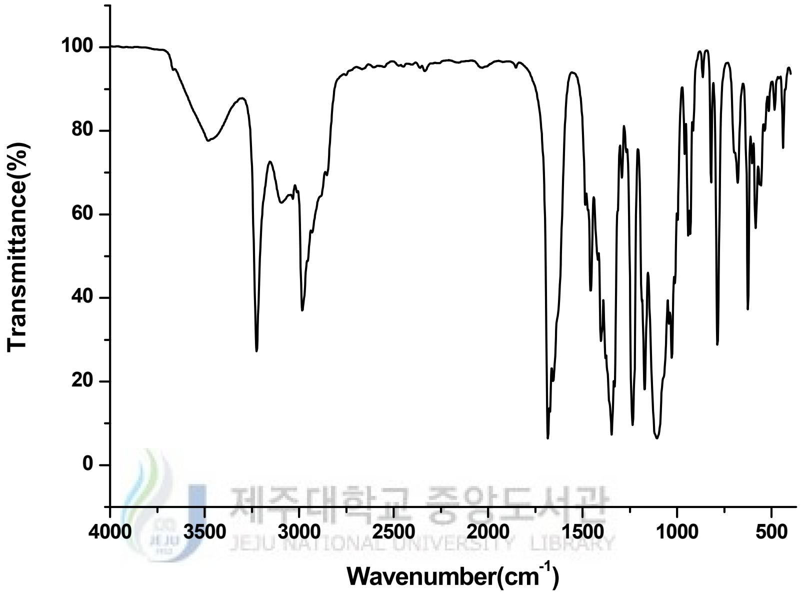

Fig. 14. IR spectrum of *cis*-[Cr([14]-decane)(ca)$_2$]ClO_4.

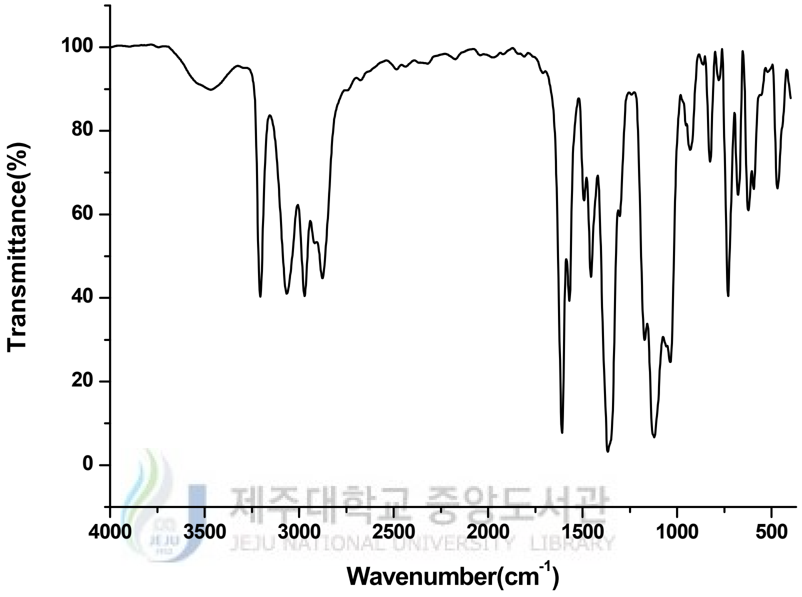

Fig. 15. IR spectrum of *cis*-[Cr([14]-decane)(bz)$_2$]ClO$_4$ · 0.5H$_2$O.

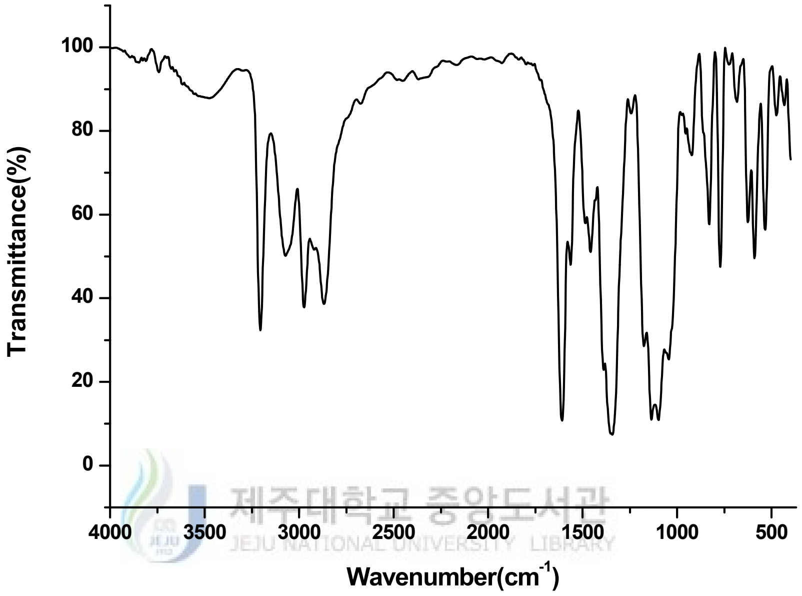

Fig. 16. IR spectrum of *cis*-[Cr([14]-decane)(cbz)$_2$]ClO$_4$.

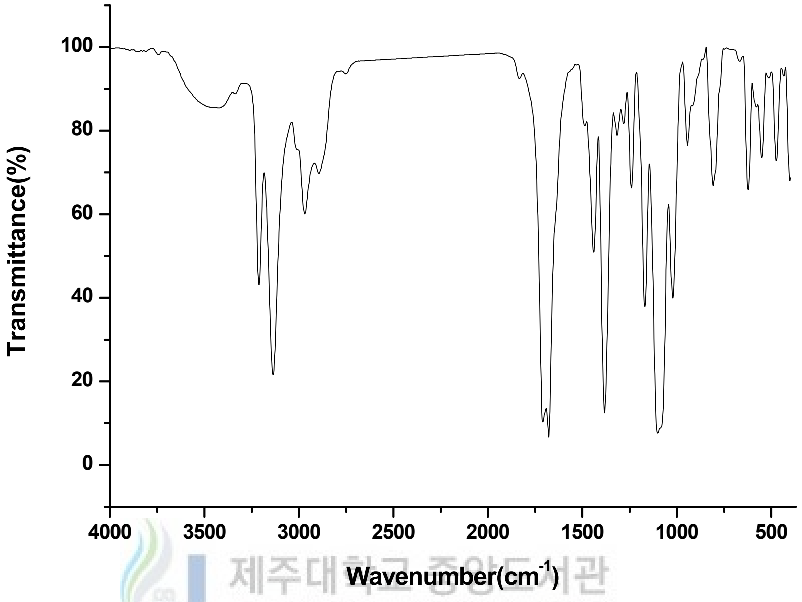

Fig. 17. IR spectrum of *cis*-[Cr([14]-decane)(ox)]$ClO_4 \cdot 0.5H_2O$.

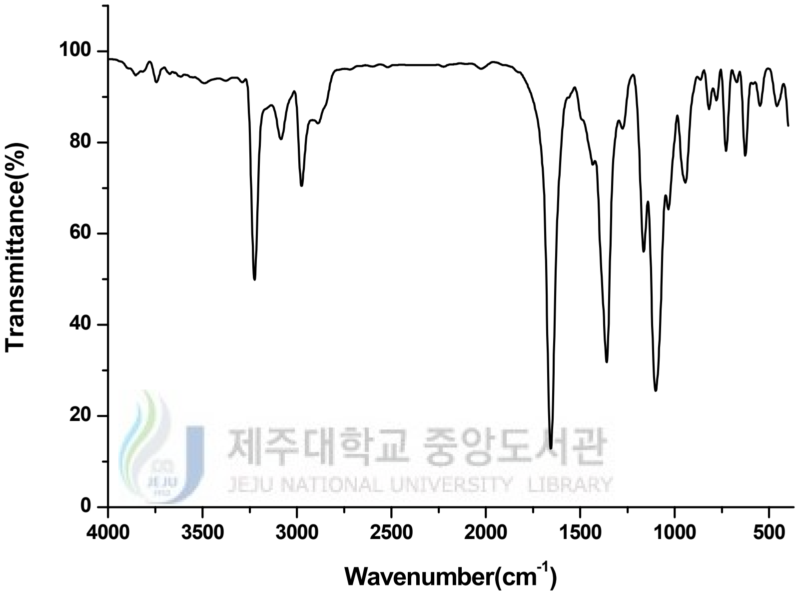

Fig. 18. IR spectrum of *cis*-[Cr([14]-decane)(mal)]$ClO_4 \cdot 0.25H_2O$.

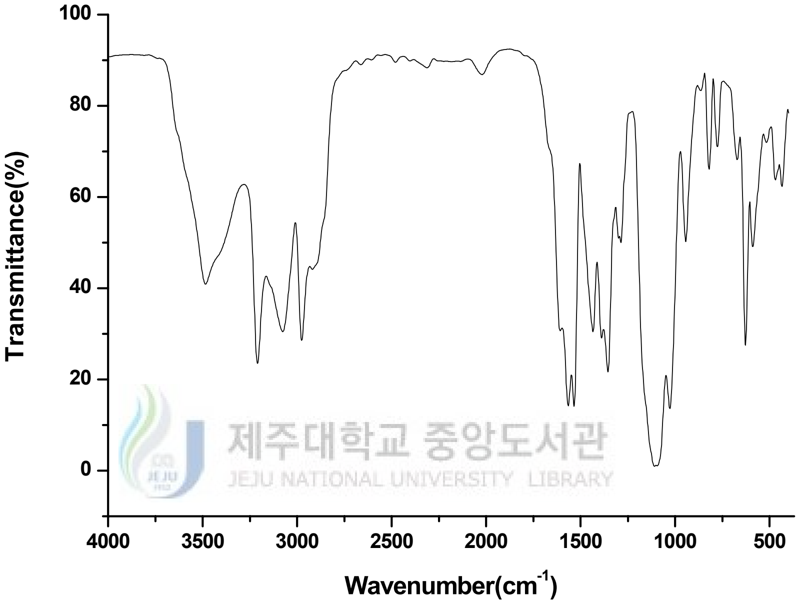

Fig. 19. IR spectrum of *cis*-[Cr([14]-decane)(acac)]$(ClO_4)_2 \cdot 0.5H_2O$.

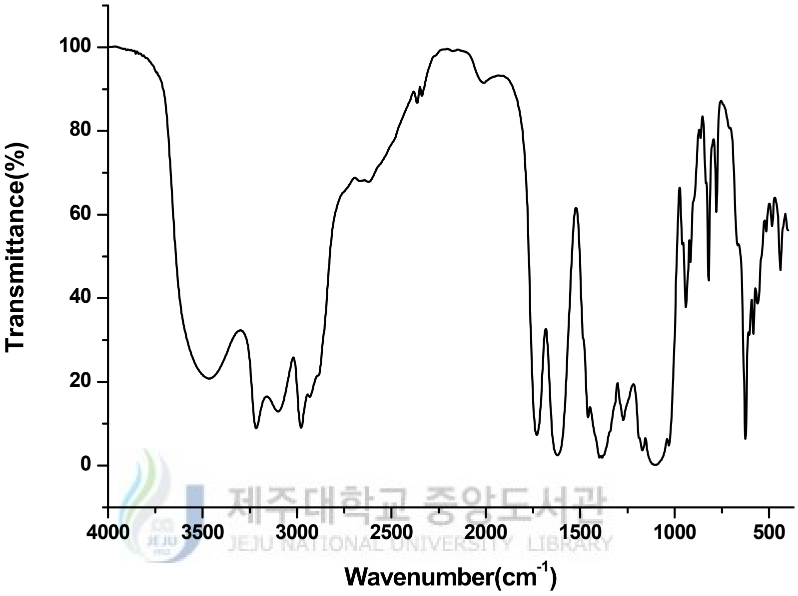

Fig. 20. IR spectrum of *cis*-[{Cr([14]-decane)(μ-cit)}$_2$](ClO$_4$)$_2$ · 6H$_2$O.

4. FAB Mass Spectrometry

The FAB mass spectra of the complexes were shown in Fig. 21～29, and summarized at Table 14. The FAB mass spectra peaks of all complexes were corresponding to the molecular ion [Cr([14]-decane)$(L_a)_m]^+$ (m = 1 or 2). The complexes of two coordinated auxiliary ligands generated two peaks to the species [Cr([14]-decane)$(L_a)]^+$ and [Cr([14]-decane)$(L_a)_2]^+$ {NCS^- : m/z 394, 452 ; N_3^- : 377, 420 ; benzonate (bz) : m/z 456, 578 ; p-chlorobenzonate (cbz) : m/z 490, 646 ; chloroacetate (ca) : m/z 428, 522}. The FAB mass spectrum of the oxalate complex [Cr([14]-decane)(ox)]$ClO_4 \cdot 0.5H_2O$ showed a peak at m/z 424 corresponding to the molecular ion [Cr([14]-decane)(ox)]$^+$. The molecular ion lost the exocyclic ligand (ox ; $C_2O_4^{2-}$) which revealed the formation of the fragment [Cr([14]-decane)-H]$^+$ at m/z 335. This fragment was well observed in the FAB mass spectra of all complexes. The mass spectrum of the malonate complex [Cr([14]-decane)(mal)]$ClO_4 \cdot 0.25H_2O$ showed a peak at m/z 438, which was corresponding to the molecular ion [Cr([14]-decane)(mal)]$^+$. In the mass spectrum of the acetylacetonate complex [Cr([14]-decane)-(acac)]$(ClO_4) \cdot 0.5H_2O$, peaks at m/z 434 and 534 were due to the species [Cr([14]-decane)(acac)-2H]$^+$ and [Cr([14]-decane)(acac)

$-(ClO_4)-H]^+$, respectively. In the FAB mass spectrum of $[\{Cr([14]\text{-decane})(\mu\text{-cit})\}_2](ClO_4)_2 \cdot 6H_2O$, peak corresponding to bridged complex ion of the $[\{Cr([14]\text{-decane})(\mu\text{-cit})\}_2]^+$ type([4]) was observed at m/z 1053. Peaks at *m/z* 526 and 718 were due to the species $[Cr([14]\text{-decane})(cit)]^+$ and $[Cr([14]\text{-decane})(cit)_2]^+$, respectively.

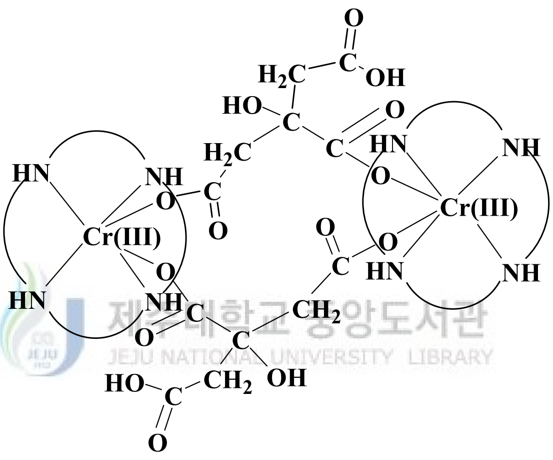

[4]

Table 14. FAB Mass Spectral Data of the Cr(III) Complexes.

complex	m/z	Fragments
$[Cr([14]\text{-decane})(NCS)_2]ClO_4 \cdot H_2O$	335	$[Cr([14]\text{-decane})\text{-}H]^+$
	394	$[Cr([14]\text{-decane})(NCS)]^+$
	452	$[Cr([14]\text{-decane})(NCS)_2\text{-}H]^+$
$[Cr([14]\text{-decane})(N_3)_2]ClO_4$	335	$[Cr([14]\text{-decane})\text{-}H]^+$
	377	$[Cr([14]\text{-decane})(N_3)\text{-}H]^+$
	420	$[Cr([14]\text{-decane})(N_3)_2\text{-}H]^+$
	349	$[Cr([14]\text{-decane})(N)\text{-}H]^+$
$[Cr([14]\text{-decane})(ca)_2]ClO_4$	335	$[Cr([14]\text{-decane})\text{-}H]^+$
	428	$[Cr([14]\text{-decane})(ca)\text{-}2H]^+$
	522	$[Cr([14]\text{-decane})(ca)_2\text{-}2H]^+$
$[Cr([14]\text{-decane})(bz)_2]ClO_4 \cdot 0.5H_2O$	335	$[Cr([14]\text{-decane})\text{-}H]^+$
	456	$[Cr([14]\text{-decane})(bz)\text{-}2H]^+$
	578	$[Cr([14]\text{-decane})(bz)_2\text{-}H]^+$

Table 14. *Continued*

complex	m/z	Fragments
$[Cr([14]\text{-decane})(cbz)_2]ClO_4$	334	$[Cr([14]\text{-decane})-2H]^+$
	490	$[Cr([14]\text{-decane})(cbz)-2H]^+$
	646	$[Cr([14]\text{-decane})(cbz)_2-2H]^+$
$[Cr([14]\text{-decane})(ox)]ClO_4 \cdot 0.5H_2O$	335	$[Cr([14]\text{-decane})-H]^+$
	424	$[Cr([14]\text{-decane})(ox)]^+$
$[Cr([14]\text{-decane})(mal)]ClO_4 \cdot 0.25H_2O$	335	$[Cr([14]\text{-decane})-H]^+$
	438	$[Cr([14]\text{-decane})(mal)]^+$
$[Cr([14]\text{-decane})(acac)](ClO_4)_2 \cdot 0.5H_2O$	333	$[Cr([14]\text{-decane})-3H]^+$
	434	$[Cr([14]\text{-decane})(acac)-2H]^+$
	534	$[Cr([14]\text{-decane})(acac)(ClO_4)-H]^+$
$[\{Cr([14]\text{-decane})(\mu\text{-cit})\}_2](ClO_4)_2 \cdot 6H_2O$	335	$[Cr([14]\text{-decane})-H]^+$
	526	$[Cr([14]\text{-decane})(cit)-H]^+$
	718	$[Cr([14]\text{-decane})(cit)_2+H]^+$
	1053	$[Cr([14]\text{-decane})(cit)]_2^+$

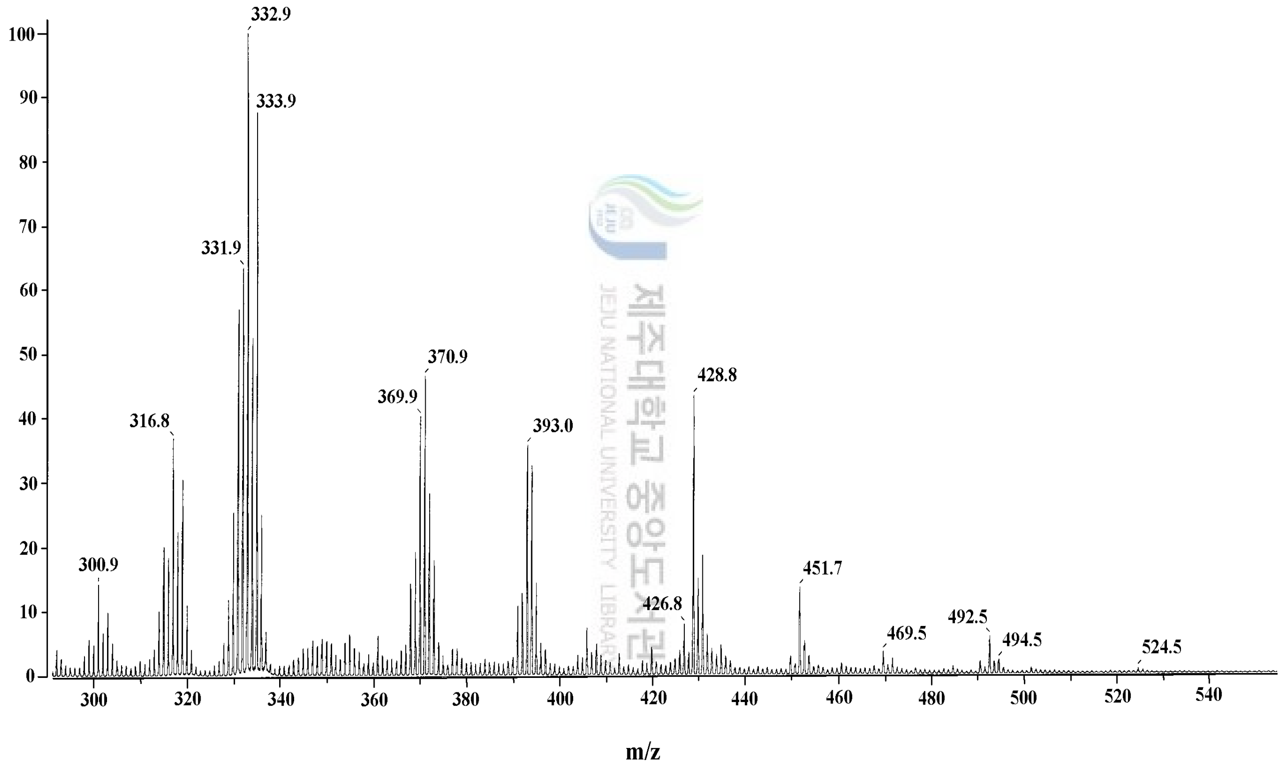

Fig. 21. FAB mass spectrum of the *cis*-[Cr([14]-decane)$(NCS)_2$]$ClO_4 \cdot H_2O$.

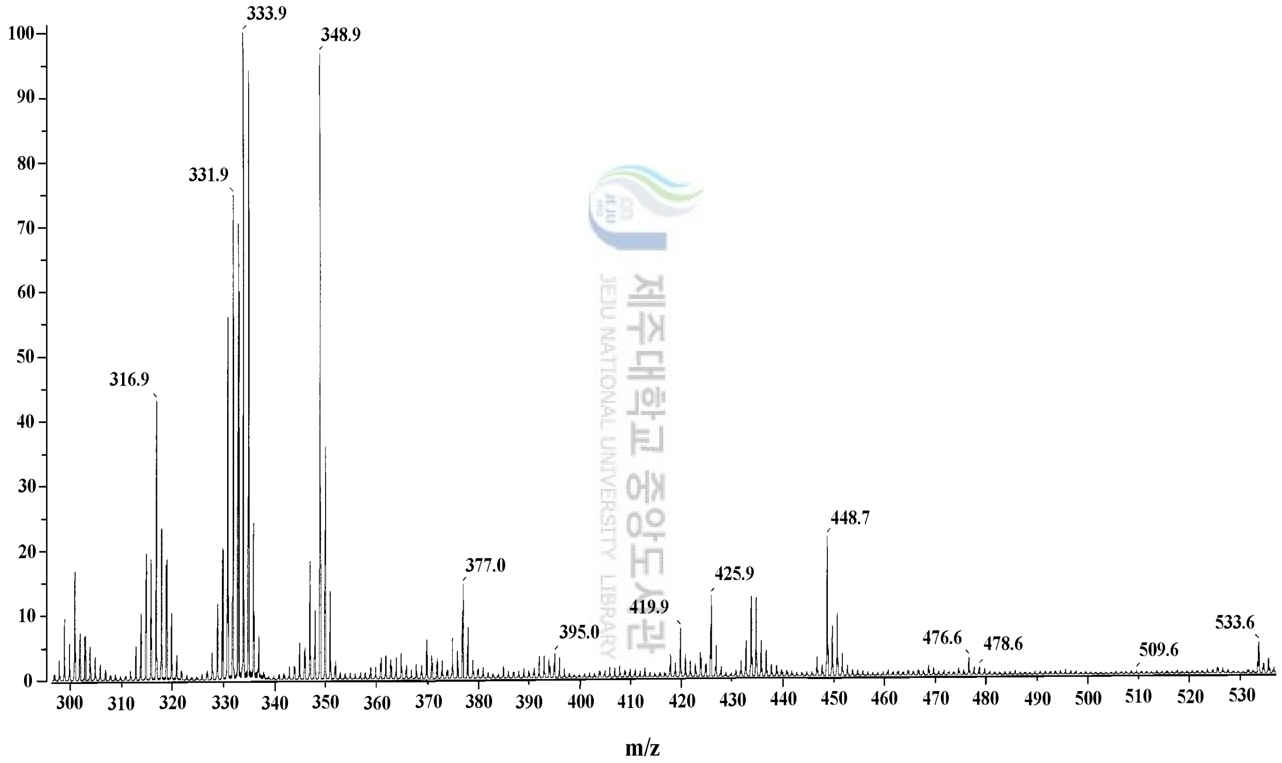

Fig. 22. FAB mass spectrum of the *cis*-[Cr([14]-decane)$(N_3)_2$]ClO_4.

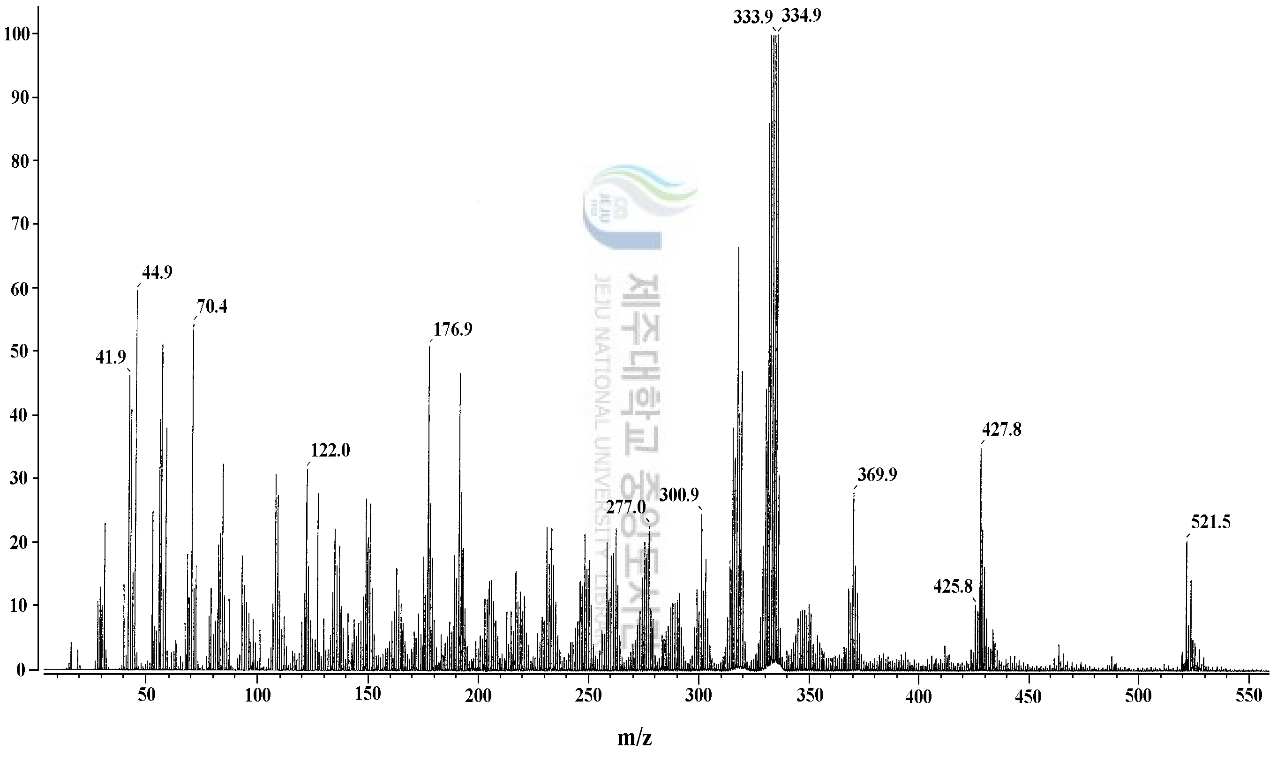

Fig. 23. FAB mass spectrum of the *cis*-[Cr([14]-decane)(ca)$_2$]ClO$_4$.

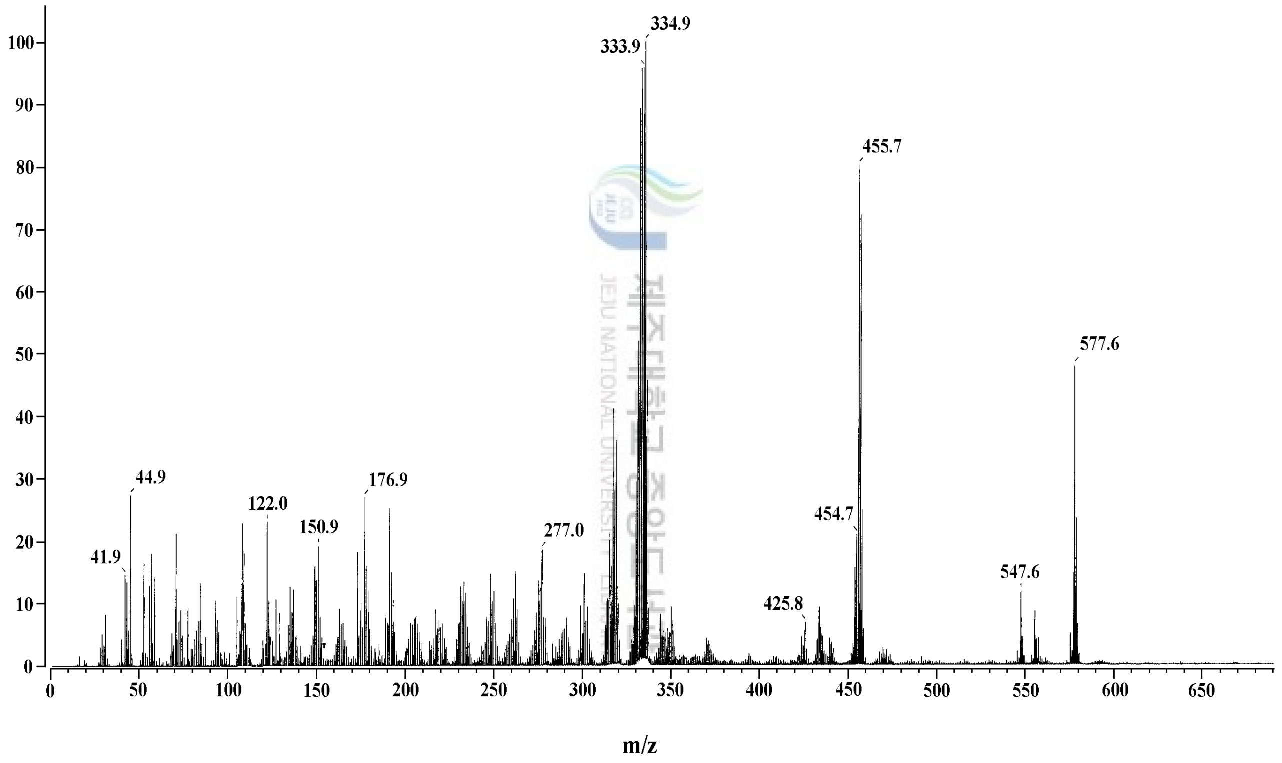

Fig. 24. FAB mass spectrum of the *cis*-[Cr([14]-decane)(bz)$_2$]ClO$_4$ · 0.5H$_2$O.

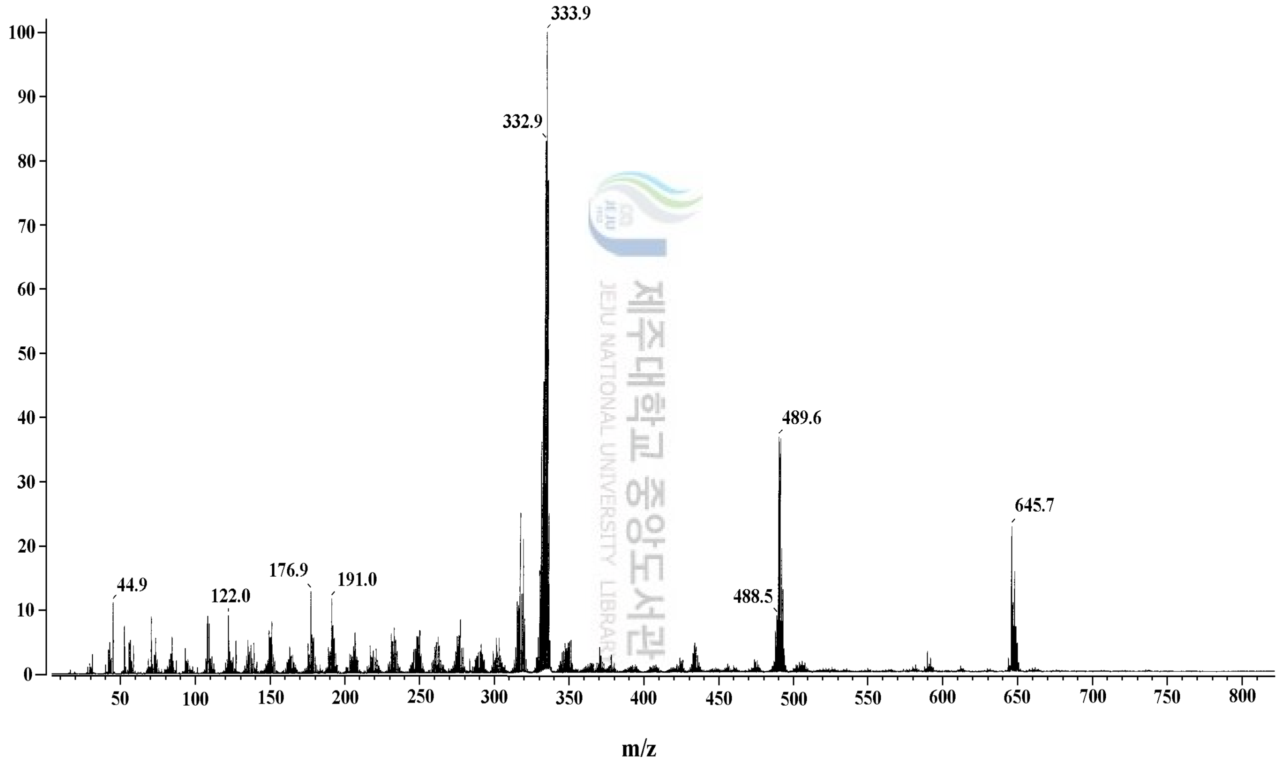

Fig. 25. FAB mass spectrum of the *cis*-[Cr([14]-decane)(cbz)$_2$]ClO$_4$.

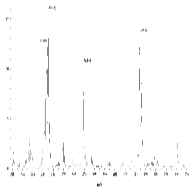

Fig. 26. FAB mass spectrum of the *cis*-[Cr([14]-decane)(ox)]$ClO_4 \cdot 0.5H_2O$.

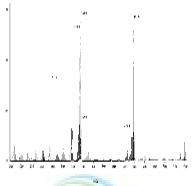

Fig. 27. FAB mass spectrum of the *cis*-[Cr([14]-decane)(mal)]$ClO_4 \cdot 0.25H_2O$.

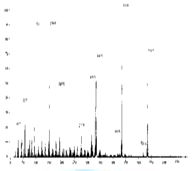

Fig. 28. FAB mass spectrum of the *cis*-[Cr([14]-decane)(acac)]$(ClO_4)_2 \cdot 0.5H_2O$.

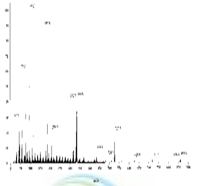

Fig. 29(a). FAB mass spectrum of the *cis*-[{Cr([14]-decane)(μ-cit)}$_2$](ClO$_4$)$_2$ · 6H$_2$O.

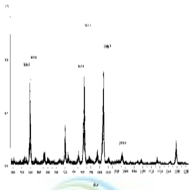

Fig. 29(b). FAB mass spectrum of the *cis*-$[\{Cr([14]\text{-decane})(\mu\text{-citrato})\}_2](ClO_4)_2 \cdot 6H_2O$.

5. Thermogravimetry

Thermogravimetry analysis(TGA) have been carried out simultaneously for the Cr(III) complexes of [14]-decane ligand (Fig. 30~38). Thermogravimetric details were given in Table 15. It was found out from the results that the prepared macrocycle compounds have relatively high thermal stability. Bidentate oxalate and malonate ions were lost at 250~350℃ range. Along with the removal of the those ion in the range of temperature, the perchlorate ion had also been removed. In acetylacetonate complex, two perchlorate ions were lost at 245~292℃, and then coordinated acetylacetonate removed in the range of 292~349℃. In Cr(III) complexes with monodentate ligands such as bezonate, *p*-chlorobenzonate, chloroacetate and azide were lost stepwise in 200~350℃. And the perchlorate ion also removed at this temperature.

In $[\{Cr([14]\text{-decane})(\mu\text{-cit})\}_2](ClO_4)_2 \cdot 6H_2O$ complex, lattice water molecules were removed at near 210℃. After two perchlorate and one coordinated citrate ion were lost at 210~283℃, and then one coordinated citrate ion removed at 283~357℃. The macrocyclic entity changed slowly up to 350℃, and then those complexes have been changed to green Cr_2O_3 were observed at over 990℃.

$[\{Cr([14]\text{-}decane)(\mu\text{-}cit)\}_2](ClO_4)_2 \cdot 6H_2O$

$\downarrow$ ~210℃

- lattice $6H_2O$(Obs. 7.84%, Calc. 7.95%)

$[\{Cr([14]\text{-}decane)(\mu\text{-}cit)\}_2](ClO_4)_2$

$\downarrow$ 210~283℃

- $2ClO_4^-$ + cit^{2-}(Obs. 28.18%, Calc. 28.32%)

$[\{Cr([14]\text{-}decane)\}_2(\mu\text{-}cit)]$

$\downarrow$ 283~357℃

- cit^{2-}(Obs. 12.41%, Calc. 13.69%)

$[\{Cr([14]\text{-}decane)\}_2]$

$\downarrow$ 357℃~

- macrocyclic ligand

Cr_2O_3

Scheme 2. The proposed decomposition stages for $[\{Cr([14]\text{-}decane)(\mu\text{-}cit)\}_2](ClO_4)_2 \cdot 6H_2O$.

Table 15. Thermogravimetric Data of the Cr(III) Complexes

complexes	temperature range (℃)	Moieties lost
$[Cr([14]\text{-decane})(NCS)_2]ClO_4 \cdot H_2O$	246～278	ClO_4^-
	278～346	coordinate $2NCS^-$
	346～990	macrocyclic ligand
$[Cr([14]\text{-decane})(N_3)_2]ClO_4$	183～273	ClO_4^- + coordinate N_3^-
	273～346	coordinate N_3^-
	345～990	macrocyclic ligand
$[Cr([14]\text{-decane})(ca)_2]ClO_4$	207～291	ClO_4^- + coordinate ca^-
	291～348	coordinate ca^-
	348～990	macrocyclic ligand
$[Cr([14]\text{-decane})(bz)_2]ClO_4 \cdot 0.5H_2O$	257～306	ClO_4^- + coordinate bz^-
	306～408	coordinate bz^-
	408～990	marocyclic ligand

Table 15. *Continued*

complex	temperature range (℃)	Moieties lost
$[Cr([14]\text{-}decane)(cbz)_2]ClO_4$	239～317	ClO_4^- + coordinate cbz^-
	317～415	coordinate cbz^-
	415～990	marocyclic ligand
$[Cr([14]\text{-}decane)(ox)]ClO_4 \cdot 0.5H_2O$	248～348	ClO_4^- + coordinate ox^{2-}
	348～985	marocyclic ligand
$[Cr([14]\text{-}decane)(mal)]ClO_4 \cdot 0.25H_2O$	269～310	ClO_4^- + coordinate mal^{2-}
	310～975	marocyclic ligand
$[Cr([14]\text{-}decane)(acac)](ClO_4)_2 \cdot 0.5H_2O$	245～292	$2ClO_4^-$
	292～349	coordinate $acac^-$
	349～990	marocyclic ligand
$[\{Cr([14]\text{-}decane)(\mu\text{-}cit)\}_2](ClO_4)_2 \cdot 6H_2O$	～210	lattice $6H_2O$
	210～283	ClO_4^- + coordinate cit^-
	283～357	coordinate cit^-
	357～990	macrocyclic ligand

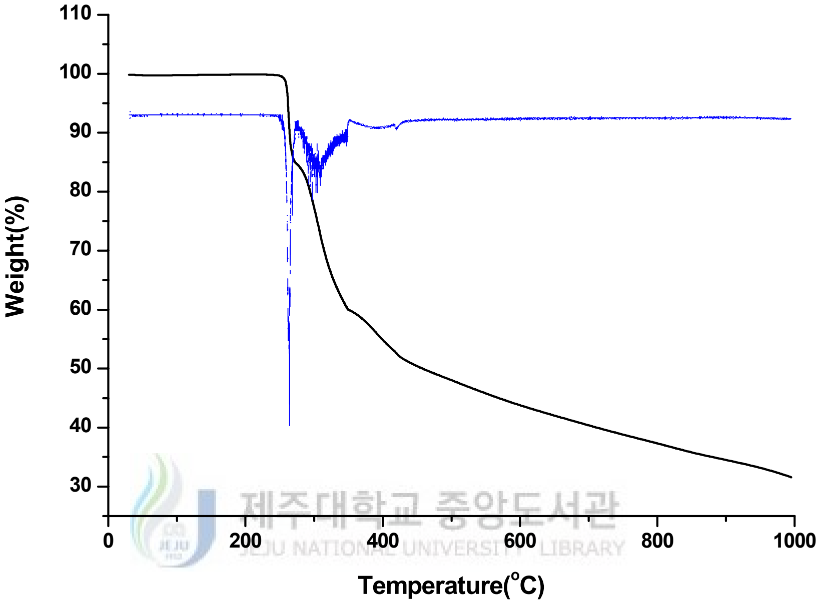

Fig. 30. Thermogravimetric curve (solid line) and second derivative (dashed line) of *cis*-[Cr([14]-decane)(NCS)$_2$]ClO$_4$ · H$_2$O.

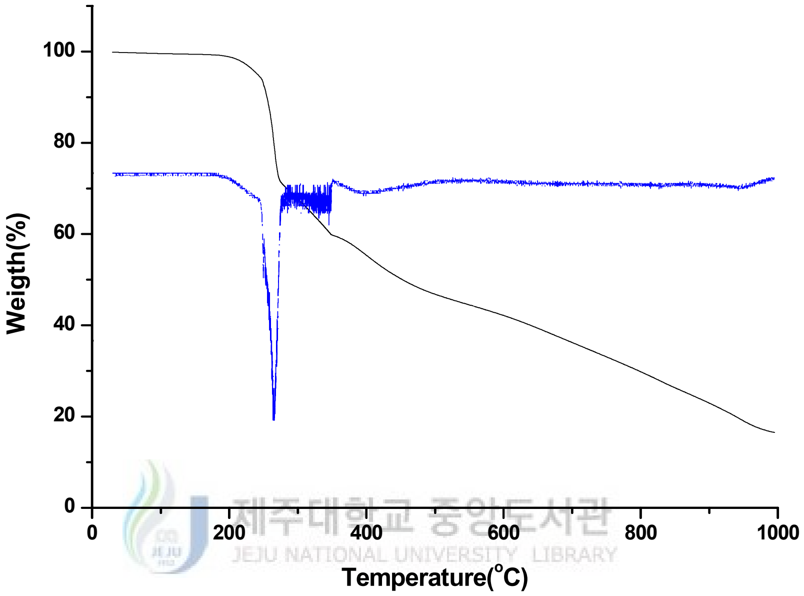

Fig. 31. Thermogravimetric curve (solid line) and second derivative (dashed line) of *cis*-[Cr([14]-decane)$(N_3)_2$]ClO_4.

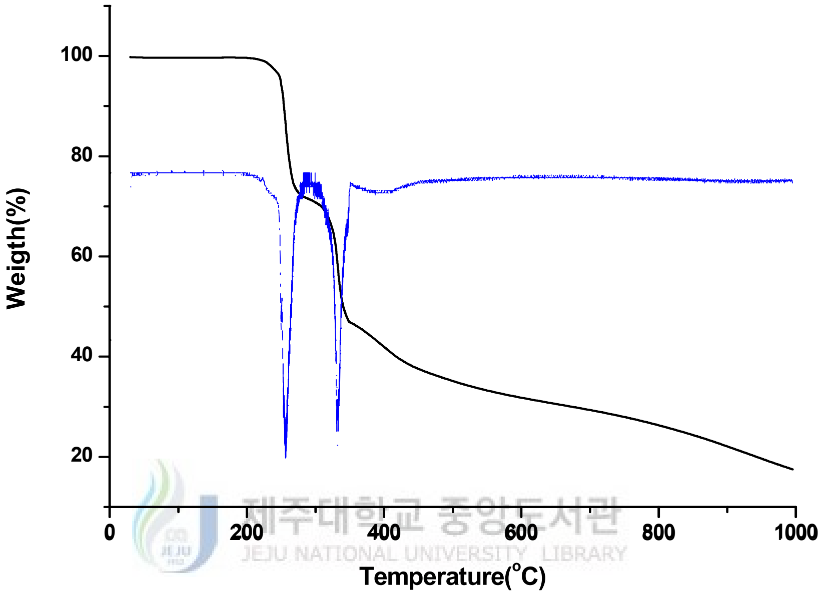

Fig. 32. Thermogravimetric curve (solid line) and second derivative (dashed line) of *cis*-[Cr([14]-decane)(ca)$_2$]ClO$_4$.

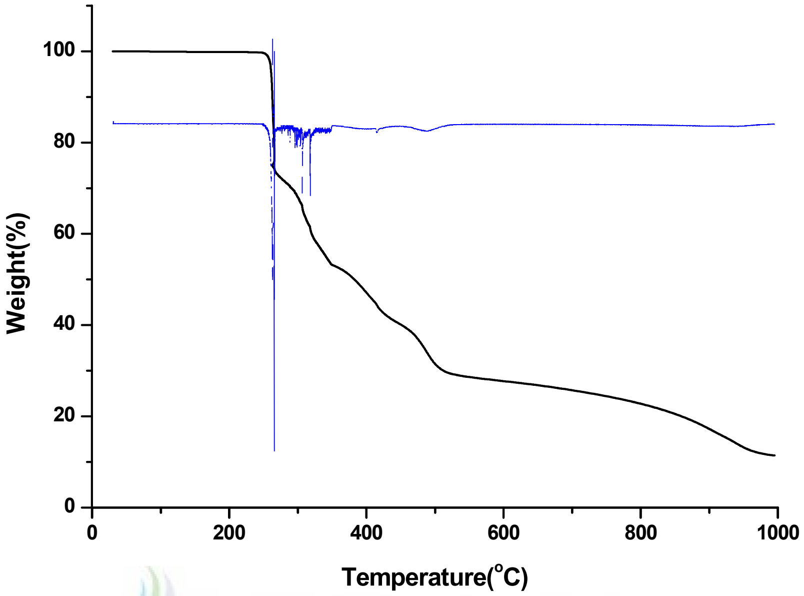

Fig. 33. Thermogravimetric curve (solid line) and second derivative (dashed line) of *cis*-$[Cr([14]\text{-decane})(bz)_2]ClO_4 \cdot 0.5H_2O$.

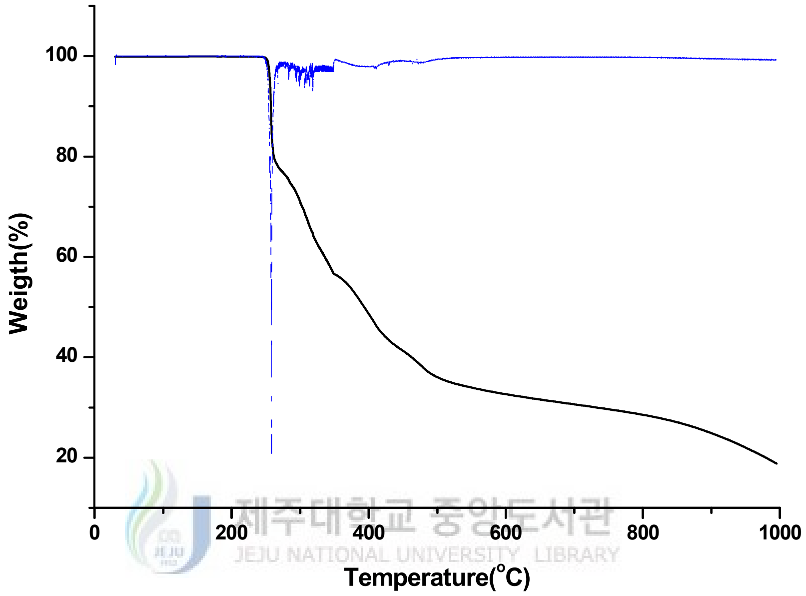

Fig. 34. Thermogravimetric curve (solid line) and second derivative (dashed line) of *cis*-[Cr([14]-decane)(cbz)$_2$]ClO$_4$.

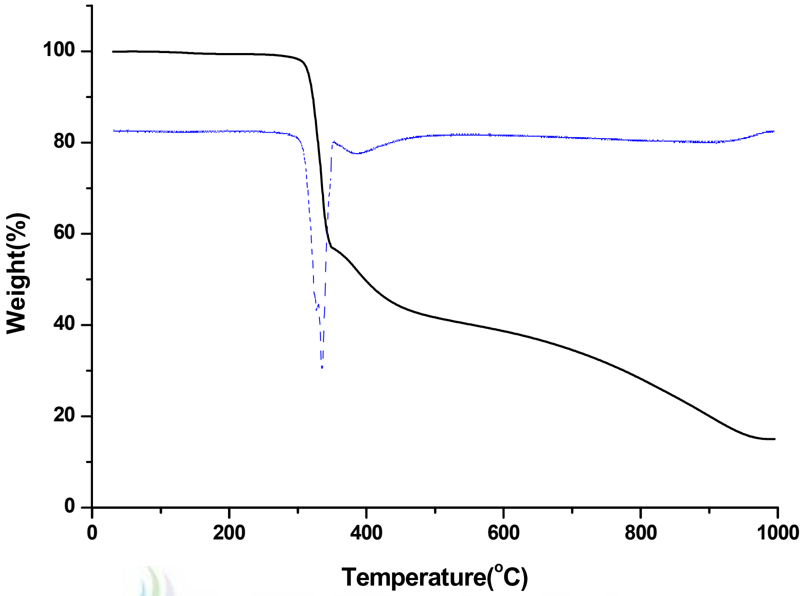

Fig. 35. Thermogravimetric curve (solid line) and second derivative (dashed line) of *cis*-[Cr([14]-decane)(ox)]$ClO_4 \cdot 0.5H_2O$.

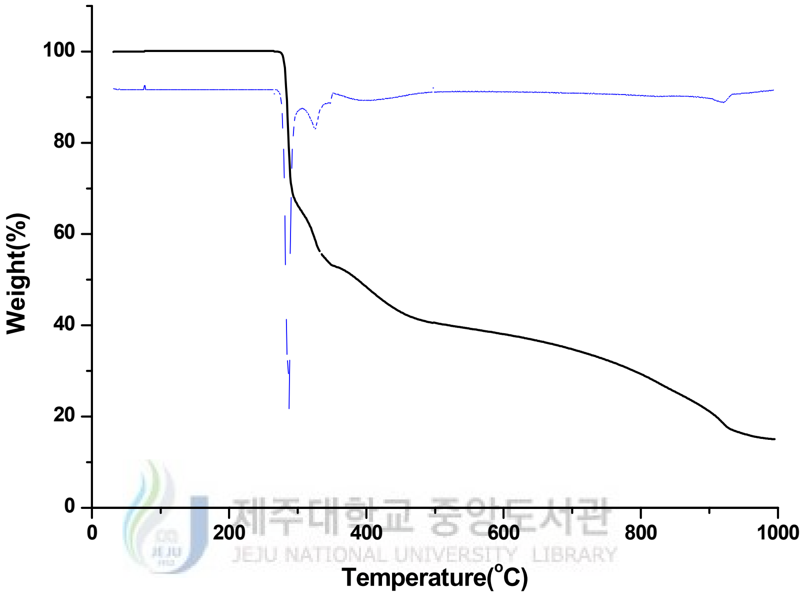

Fig. 36. Thermogravimetric curve (solid line) and second derivative (dashed line) of *cis*-[Cr([14]-decane)(mal)]$ClO_4 \cdot 0.25H_2O$.

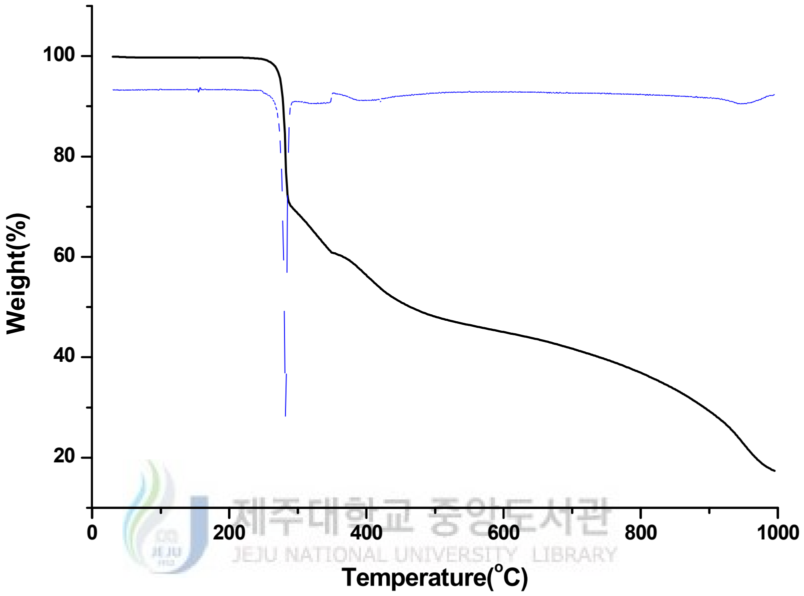

Fig. 37. Thermogravimetric curve (solid line) and second derivative (dashed line) of *cis*-[Cr([14]-decane)(acac)]$(ClO_4)_2 \cdot 0.5H_2O$.

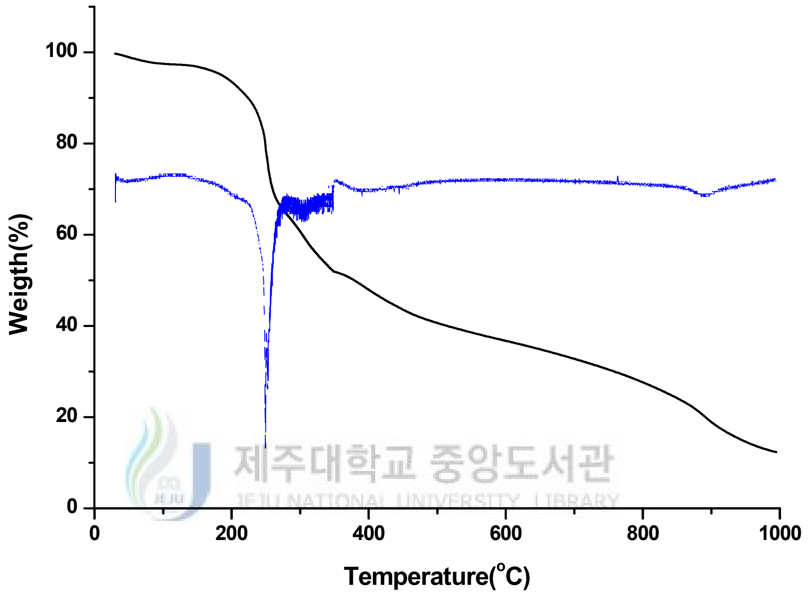

Fig. 38. Thermogravimetric curve (solid line) and second derivative (dashed line) of *cis*-$[Cr([14]\text{-decane})(\mu\text{-cit})]_2(ClO_4)_2 \cdot 6H_2O$.

6. Structure Analysis

1) Crystal Structure of *cis*-$[Cr([14]\text{-decane})(NCS)_2]ClO_4 \cdot H_2O$

The structure of the *cis*-$[Cr([14]\text{-decane})(NCS)_2]ClO_4 \cdot H_2O$ with the atomic labeling was depicted in Fig. 39. The figure was drawn by ORTEP program at 30% probability level. Table 16 and 17 showed the selected bond distances and bond angles.

The structure analysis indicated that the crystal consists of di(isothiocyanato)([14]-decane)chromium(III) mono-cation and perchlorate ion in the molecular ratio of 1:1, formulated as $[Cr([14]\text{-decane})(NCS)_2]ClO_4 \cdot H_2O$. This was well fitted with elemental analysis results. The hexacoordination geometry around Cr(III) ion exhibited a distorted octahedral structure {$CrN_2N'_2$ (N′-*NCS*)-plane and two N (*C-dimethyl*) group of its z-axis}. In this complex Cr(III) was coordinated with the four secondary nitrogen atoms of the macrocycle and two nitrogen atom of two isothiocyanate in the *cis* position. The Cr-N′(-*NCS*) {Cr-N(5); 1.964Å, Cr-N(6); 2.000Å} bond distances were shorter than Cr-N (*macrocycle*) bond distances {Cr-N(2); 2.103Å, Cr-N(4); 2.104Å, Cr-N(3); 2.132Å, Cr-N(4); 2.147Å}. The Cr-N (*C-dimethyl*) bond distances were slightly longer (average 0.036 Å) than the Cr-N

(*C-methyl*) bond distances. The N-C-S bond angles of coordinated Cr(III) were similar line: ∠N(5)-C(17)-S(1) = 178.1(5)°, ∠N(6)-C(18)-S(2) = 177.3(6)°. The bond angles about the Cr-N=CS {∠C(17)-N(5)-Cr = 165.0(4)°, ∠C(18)-N(6)-Cr = 167.3(5)°} deviated from 180°caused by nonbonding electron pair of nitrogen atom. This revealed nitrogen atom was bonded to Cr ion.

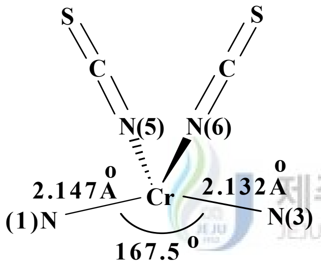

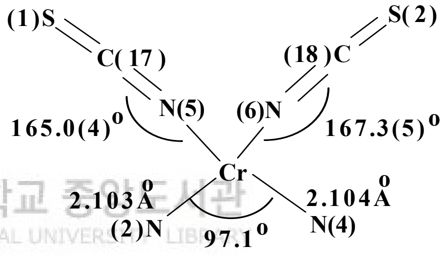

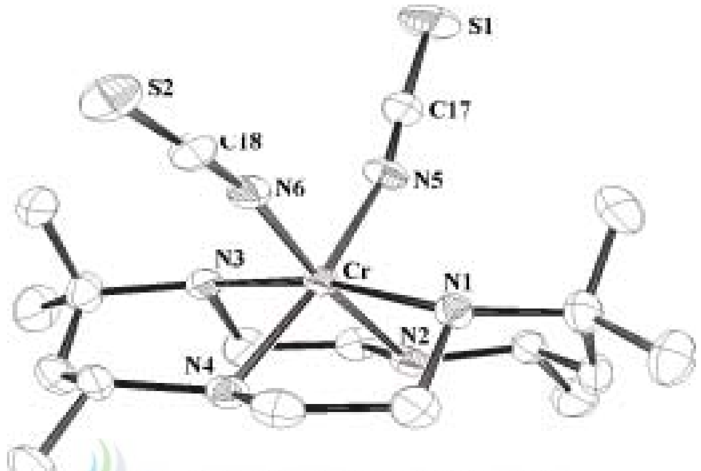

Fig. 39. ORTEP plot of the *cis*-$[Cr([14]\text{-decane})(NCS)_2]ClO_4 \cdot H_2O$ complex.

Table 16. Selected Bond Lengths (Å) for *cis*-$[Cr([14]\text{-decane})\text{-}(NCS)_2]ClO_4 \cdot H_2O$

Cr(1)-N(5)	1.964(5)	C(1)-C(4)	1.525(9)
Cr(1)-N(6)	2.000(5)	C(1)-C(3)	1.563(8)
Cr(1)-N(2)	2.103(4)	C(4)-C(5)	1.523(9)
Cr(1)-N(4)	2.104(4)	C(5)-C(6)	1.526(8)
Cr(1)-N(3)	2.132(4)	C(7)-C(8)	1.497(8)
Cr(1)-N(1)	2.147(4)	C(9)-C(12)	1.506(8)
N(1)-C(16)	1.482(7)	C(9)-C(10)	1.512(9)
N(1)-C(1)	1.502(7)	C(9)-C(11)	1.545(8)
N(2)-C(7)	1.501(7)	C(12)-C(13)	1.538(8)
N(2)-C(5)	1.508(6)	C(13)-C(14)	1.536(7)
N(3)-C(8)	1.522(7)	C(15)-C(16)	1.479(8)
N(3)-C(9)	1.522(7)	C(17)-S(1)	1.589(7)
N(4)-C(13)	1.499(6)	C(18)-S(2)	1.632(7)
N(4)-C(15)	1.503(7)	Cl(1)-O(4)	1.359(4)
N(5)-C(17)	1.216(7)	Cl(1)-O(3)	1.382(6)
N(6)-C(18)	1.139(7)	Cl(1)-O(2)	1.420(7)
C(1)-C(2)	1.515(8)	Cl(1)-O(1)	1.433(6)

Table 17. Selected Bond Angles (°) for *cis*-[Cr([14]-decane)-$(NCS)_2]ClO_4 \cdot H_2O$

N(5)-Cr(1)-N(6)	88.0(2)	C(8)-N(3)-Cr(1)	105.6(3)
N(5)-Cr(1)-N(2)	87.3(2)	C(9)-N(3)-Cr(1)	122.7(3)
N(6)-Cr(1)-N(2)	172.4(2)	C(13)-N(4)-C(15)	110.9(4)
N(5)-Cr(1)-N(4)	172.8(2)	C(13)-N(4)-Cr(1)	117.1(3)
N(6)-Cr(1)-N(4)	88.2(2)	C(15)-N(4)-Cr(1)	105.5(3)
N(2)-Cr(1)-N(4)	97.1(2)	C(17)-N(5)-Cr(1)	165.0(4)
N(5)-Cr(1)-N(3)	87.3(2)	C(18)-N(6)-Cr(1)	167.3(5)
N(6)-Cr(1)-N(3)	100.9(2)	N(1)-C(1)-C(2)	108.6(5)
N(2)-Cr(1)-N(3)	84.8(2)	N(1)-C(1)-C(4)	109.6(5)
N(4)-Cr(1)-N(3)	87.4(2)	C(2)-C(1)-C(4)	111.0(6)
N(5)-Cr(1)-N(1)	102.5(2)	N(1)-C(1)-C(3)	110.1(5)
N(6)-Cr(1)-N(1)	87.3(2)	C(2)-C(1)-C(3)	109.1(5)
N(2)-Cr(1)-N(1)	87.9(2)	C(4)-C(1)-C(3)	108.4(5)
N(4)-Cr(1)-N(1)	83.4(2)	C(5)-C(4)-C(1)	120.7(5)
N(3)-Cr(1)-N(1)	167.5(2)	N(2)-C(5)-C(4)	110.2(5)
C(16)-N(1)-C(1)	111.4(4)	N(2)-C(5)-C(6)	111.2(5)
C(16)-N(1)-Cr(1)	106.5(3)	C(4)-C(5)-C(6)	112.1(5)
C(1)-N(1)-Cr(1)	122.7(4)	C(8)-C(7)-N(2)	109.4(5)
C(16)-N(1)-H(1)	104.9(3)	C(7)-C(8)-N(3)	110.3(5)
C(7)-N(2)-C(5)	111.5(4)	C(12)-C(9)-C(10)	114.1(6)
C(7)-N(2)-Cr(1)	105.3(3)	C(12)-C(9)-N(3)	110.7(4)
C(5)-N(2)-Cr(1)	117.6(3)	C(10)-C(9)-N(3)	107.3(5)
C(8)-N(3)-C(9)	112.6(4)	N(3)-C(9)-C(11)	111.6(5)

Table 17. *Continued*

C(9)-C(12)-C(13)	117.8(5)	N(6)-C(18)-S(2)	177.3(6)
N(4)-C(13)-C(14)	113.4(4)	O(4)-Cl(1)-O(3)	125.6(5)
N(4)-C(13)-C(12)	111.8(5)	O(4)-Cl(1)-O(2)	102.2(5)
C(14)-C(13)-C(12)	107.4(5)	O(3)-Cl(1)-O(2)	107.3(6)
C(16)-C(15)-N(4)	109.4(5)	O(4)-Cl(1)-O(1)	109.4(4)
C(15)-C(16)-N(1)	110.3(4)	O(3)-Cl(1)-O(1)	101.4(5)
N(5)-C(17)-S(1)	178.1(5)	O(2)-Cl(1)-O(1)	110.8(5)

2) Crystal Structure of *cis*-[Cr([14]-decane)(cbz)$_2$]ClO$_4$

A perspective view of the structure of the *cis*-[Cr([14]-decane)-(cbz)$_2$]ClO$_4$ with the atomic labeling was depicted in Fig. 40. The figure was drawn by ORTEP program at 30% probability level. Table 18 and 19 exihibited the selected bond distances and bond angles. The coordinated *p*-chlorobenzoate anions were bonded to chromium via one oxygen only. The structure analysis revealed the crystal consists of di(*p*-chlorobenzoato)([14]-decane) chromium(III) mono-cation and perchlorate anion in a molecular ratio of 1:1, so formulated as [Cr([14]-decane)(cbz)$_2$]ClO$_4$. This was well fitted with elemental analysis results. The hexacoordination geometry around Cr(III) ion was a distorted octahedral {CrN$_2$O$_2$(*O-cbz*)-plane and two N (*C-dimethyl*) group of its z-axis} in which Cr(III) was coordinated with the four secondary nitrogen atoms of the macrocycle as well as with two oxygen atom of two chlorobezoate in the *cis* position. The average Cr-N bond distance was 2.126(5) Å and the average Cr-O bond distance was 1.969(4) Å. The Cr-O bond length was 1.969 Å. It compared to distances of 1.952 Å and 1.972 Å found in [Cr(edma)$_2$]$^+$ moiety and [Cr(dpt)(glygly)]ClO$_4$, respectively.[44, 45] The compound has the Cr-N bond lengths of the CrN$_4$ moiety in the range 2.115~2.140 Å, and O-Cr-O angle was 89.2(2)°. The Cr-N bond distances of this complex (average 2.126Å) were slightly longer than those of *trans*-[Cr(Me$_2$tn)$_2$Br$_2$]$^+$ moiety (from 2.078 to 2.089 Å).[46] The complex has a *cis* configuration with respected to the carboxylate oxygen. The average bond angles of five- and six-membered chelate rings around chromium(III) are known as 83.1 and 87.5°, respectively. The Cr-N (*C-dimethyl*) bond distances {Cr-N(2); 2.140(5)Å, Cr-N(4); 2,131(5)Å} were slightly longer (average 0.020 Å) than the Cr-N(*C-methyl*) bond distances{Cr-N(1); 2.115(5)Å, Cr-N(3); 2,118(5)Å}. The bond angles with the metal ion exhibited distorted octahedral angles: O(1)-Cr-O(3), O(1)-Cr-N(1), O(3)-Cr-N(3), N(1)-Cr-N(3), O(3)-Cr-N(1), O(1)-Cr-N(3) and N(4)-Cr-N(2) angles were 89.2(2)°, 87.7(2)°, 84.8(2)°, 98.4(2)°, 176.5(2)°, 173.9(2)° and 165.5(2)° respectively.

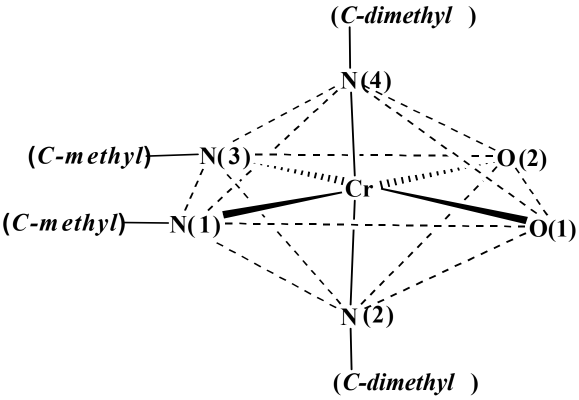

Intramolecular hydrogen bonding interactions were found between the uncoordinated carboxylate oxygen atoms of *p*-chlorobenzoic acid and the hydrogen atom of secondary amines in the macrocycle formed stable six-membered rings {O(2)···N(4) = 2.721(7)Å, ∠O(2)-H(4)-N(4) 153.5°; O(4)···N(2) = 2.791(7)Å, ∠O(4)-H(2)-N(2) 145.6°}.

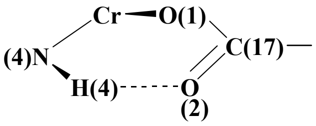

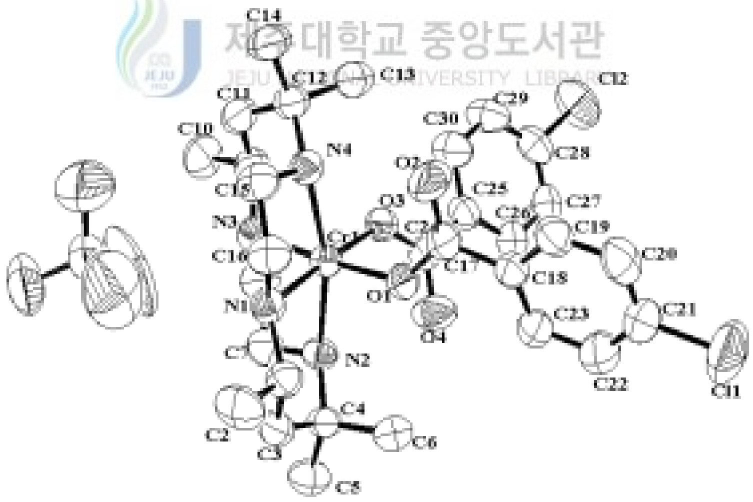

Fig. 40. ORTEP plot of the *cis*-[Cr([14]-decane)(cbz)$_2$]ClO$_4$ complex.

Table 18. Selected Bond Lengths (Å) for *cis*-[Cr([14]-decane)-(cbz)$_2$]ClO$_4$

Cr(1)-O(1)	1.964(4)	C(17)-O(2)	1.232(7)
Cr(1)-O(3)	1.973(4)	C(17)-O(1)	1.297(7)
Cr(1)-N(1)	2.115(5)	C(17)-C(18)	1.490(8)
Cr(1)-N(3)	2.118(5)	C(18)-C(23)	1.376(8)
Cr(1)-N(4)	2.131(5)	C(18)-C(19)	1.381(8)
Cr(1)-N(2)	2.140(5)	C(19)-C(20)	1.382(9)
N(1)-C(16)	1.483(7)	C(20)-C(21)	1.377(10)
N(1)-C(1)	1.502(7)	C(21)-C(22)	1.365(10)
N(2)-C(7)	1.501(7)	C(21)-Cl(1)	1.741(7)
N(2)-C(4)	1.509(7)	C(22)-C(23)	1.386(9)
N(3)-C(8)	1.482(7)	C(24)-O(4)	1.238(7)
N(3)-C(9)	1.509(7)	C(24)-O(3)	1.288(7)
N(4)-C(15)	1.473(7)	C(24)-C(25)	1.492(8)
N(4)-C(12)	1.513(7)	C(25)-C(30)	1.372(9)
C(1)-C(2)	1.550(9)	C(25)-C(26)	1.375(8)
C(3)-C(4)	1.529(8)	C(26)-C(27)	1.387(9)
C(4)-C(6)	1.519(8)	C(27)-C(28)	1.364(10)
C(4)-C(5)	1.541(8)	C(28)-C(29)	1.372(10)
C(7)-C(8)	1.495(9)	C(28)-Cl(2)	1.747(7)
C(9)-C(11)	1.525(9)	C(29)-C(30)	1.389(9)
C(9)-C(10)	1.530(9)	Cl(3)-O(5)#1	1.368(6)
C(11)-C(12)	1.529(9)	Cl(3)-O(7)	1.388(8)
C(12)-C(14)	1.537(8)	Cl(3)-O(6)	1.399(7)
C(12)-C(13)	1.538(8)	Cl(3)-O(8)	1.400(5)
C(15)-C(16)	1.492(8)	O(5)-Cl(3)#2	1.368(6)

Table 19. Selected Bond Angles (°) for *cis*-[Cr([14]-decane)(cbz)$_2$]ClO$_4$

O(1)-Cr(1)-O(3)	89.2(2)	C(8)-N(3)-Cr(1)	105.4(4)
O(1)-Cr(1)-N(1)	87.7(2)	C(9)-N(3)-Cr(1)	117.9(4)
O(3)-Cr(1)-N(1)	176.5(2)	C(15)-N(4)-C(12)	112.3(4)
O(1)-Cr(1)-N(3)	173.9(2)	C(15)-N(4)-Cr(1)	107.4(4)
O(3)-Cr(1)-N(3)	84.8(2)	C(12)-N(4)-Cr(1)	123.1(4)
N(1)-Cr(1)-N(3)	98.4(2)	N(1)-C(1)-C(3)	111.3(5)
O(1)-Cr(1)-N(4)	92.3(2)	N(1)-C(1)-C(2)	112.4(5)
O(3)-Cr(1)-N(4)	98.8(2)	C(3)-C(1)-C(2)	109.3(5)
N(1)-Cr(1)-N(4)	82.8(2)	C(1)-C(3)-C(4)	118.0(5)
N(3)-Cr(1)-N(4)	87.7(2)	N(2)-C(4)-C(6)	108.2(5)
O(1)-Cr(1)-N(2)	97.9(2)	N(2)-C(4)-C(3)	109.7(5)
O(3)-Cr(1)-N(2)	91.7(2)	C(6)-C(4)-C(3)	111.7(5)
N(1)-Cr(1)-N(2)	87.3(2)	N(2)-C(4)-C(5)	111.7(5)
N(3)-Cr(1)-N(2)	83.3(2)	C(6)-C(4)-C(5)	107.4(5)
N(4)-Cr(1)-N(2)	165.5(2)	C(3)-C(4)-C(5)	108.2(5)
C(16)-N(1)-C(1)	111.3(5)	C(8)-C(7)-N(2)	110.1(5)
C(16)-N(1)-Cr(1)	105.8(4)	N(3)-C(8)-C(7)	109.3(5)
C(1)-N(1)-Cr(1)	117.8(4)	N(3)-C(9)-C(11)	110.2(5)
C(7)-N(2)-C(4)	112.6(5)	N(3)-C(9)-C(10)	111.6(5)
C(7)-N(2)-Cr(1)	106.9(3)	C(11)-C(9)-C(10)	108.6(5)
C(4)-N(2)-Cr(1)	123.4(4)	C(9)-C(11)-C(12)	118.9(5)
C(8)-N(3)-C(9)	111.3(5)	N(4)-C(12)-C(11)	110.0(5)

Table 19. *Continued*

N(4)-C(12)-C(14)	111.8(5)	O(4)-C(24)-C(25)	118.8(6)
C(11)-C(12)-C(14)	108.4(5)	O(3)-C(24)-C(25)	117.8(6)
N(4)-C(12)-C(13)	106.9(5)	C(30)-C(25)-C(26)	119.0(6)
C(11)-C(12)-C(13)	112.5(6)	C(30)-C(25)-C(24)	122.2(6)
C(14)-C(12)-C(13)	107.2(5)	C(26)-C(25)-C(24)	118.8(6)
N(4)-C(15)-C(16)	110.8(5)	C(25)-C(26)-C(27)	121.2(7)
N(1)-C(16)-C(15)	108.5(5)	C(28)-C(27)-C(26)	118.5(7)
O(2)-C(17)-O(1)	124.0(6)	C(27)-C(28)-C(29)	121.8(7)
O(2)-C(17)-C(18)	119.1(6)	C(27)-C(28)-Cl(2)	119.2(6)
O(1)-C(17)-C(18)	116.9(6)	C(29)-C(28)-Cl(2)	119.0(6)
C(23)-C(18)-C(19)	119.1(6)	C(28)-C(29)-C(30)	118.7(7)
C(23)-C(18)-C(17)	122.3(6)	C(25)-C(30)-C(29)	120.8(7)
C(19)-C(18)-C(17)	118.6(6)	C(17)-O(1)-Cr(1)	131.8(4)
C(18)-C(19)-C(20)	121.1(7)	C(24)-O(3)-Cr(1)	128.7(4)
C(21)-C(20)-C(19)	118.4(7)	O(5)#1-Cl(3)-O(7)	103.0(7)
C(22)-C(21)-C(20)	121.6(7)	O(5)#1-Cl(3)-O(6)	112.8(6)
C(22)-C(21)-Cl(1)	119.8(6)	O(7)-Cl(3)-O(6)	104.3(6)
C(20)-C(21)-Cl(1)	118.5(6)	O(5)#1-Cl(3)-O(8)	111.3(4)
C(21)-C(22)-C(23)	119.2(7)	O(7)-Cl(3)-O(8)	110.0(5)
C(18)-C(23)-C(22)	120.6(6)	O(6)-Cl(3)-O(8)	114.5(4)
O(4)-C(24)-O(3)	123.4(6)		

3) Crystal Structure of *cis*-[Cr([14]-decane)(acac)]$(ClO_4)_2 \cdot 0.5H_2O$

A perspective view of the structure of the *cis*-[Cr([14]-decane)(acac)]$(ClO_4)_2 \cdot 0.5H_2O$ with the atomic labeling was depicted in Fig. 41. The figure was drawn by ORTEP program at 30% probability level. Table 20 and 21 revealed the selected bond distances and bond angles. The hexacoordination geometry around Cr(III) ion was a distorted octahedral {CrN_2O_2(*O-acac*)-plane and two N(*C-dimethyl*) group of its z-axis} in which Cr(III) was coordinated with the four secondary nitrogen atoms of the macrocycle as well as with two oxygen atom of bidentated acethylacetone(acac) in the *cis* position. The average distance of Cr-N and Cr-O bond were 2.121(2) Å and 1.953(2) Å, respectively. The bond distances of Cr-N(1) (2.130(3)Å) and Cr-N(3) (2.133(3) Å) were slightly longer (average 0.023 Å) than those of Cr-N(2) (2.112(3)Å) and Cr-N(4) (2.107(3)Å). The bond angles with the metal ion exhibited distorted octahedral angles : ∠N(4)-Cr-N(2), ∠O(1)-Cr-N(4), ∠N(1)-Cr-N(3), and ∠O(2)-Cr-N(4) angles were 98.69(12)°, 85.34(11)°, 169.49(12)°, and 172.94(12)°, respectively.

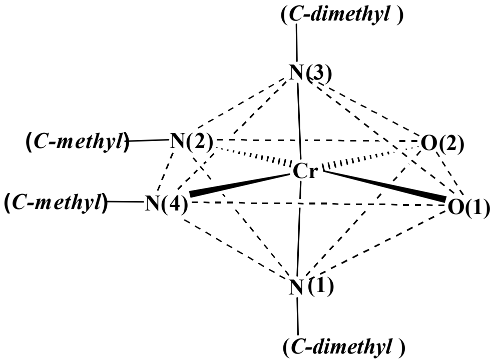

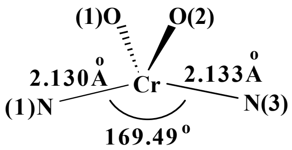

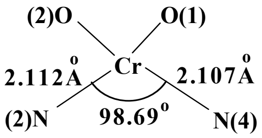

The C(18)-O(2) and C(20)-O(1) bond distances were 1.283(5) Å and 1.280(5) Å, respectively. Those distances were distinctly longer than general C=O double bond distance (1.203Å), and shorter than C-O single bond distance(1.317Å). The O(2)-Cr-O(1) angle was 89.85(11).

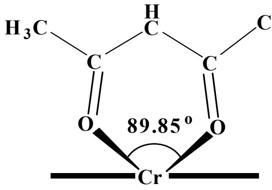

The water molecule formed hydrogen bonds with each other {O1 W⋯O1W = 2.645(45) Å}.

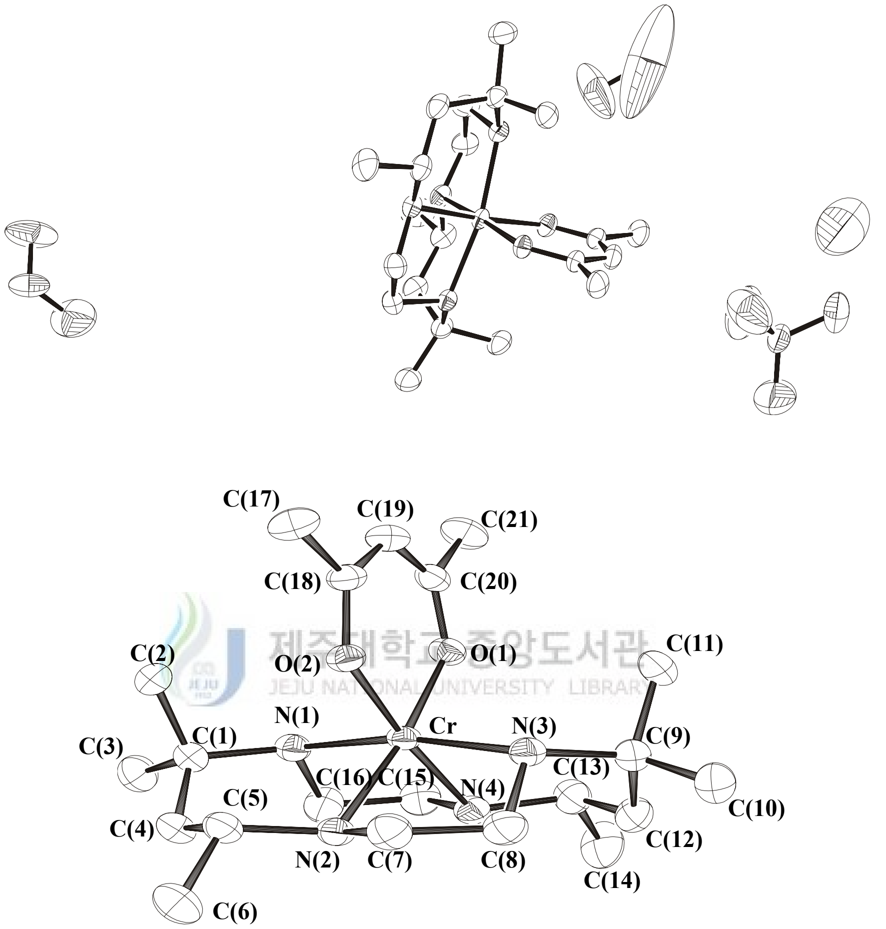

Fig. 41. ORTEP plot of the *cis*-[Cr([14]-decane)(acac)](ClO$_4$)$_2$ · 0.5 H$_2$O complex.

Table 20. Selected Bond Lengths (Å) for *cis*-[Cr([14]-decane)(acac)]$(ClO_4)_2 \cdot 0.5H_2O$

Cr(1)-O(2)	1.950(3)	C(9)-C(12)	1.534(6)
Cr(1)-O(1)	1.954(2)	C(12)-C(13)	1.526(6)
Cr(1)-N(4)	2.107(3)	C(13)-C(14)	1.529(6)
Cr(1)-N(2)	2.112(3)	C(15)-C(16)	1.498(6)
Cr(1)-N(1)	2.130(3)	C(17)-C(18)	1.505(5)
Cr(1)-N(3)	2.133(3)	C(18)-O(2)	1.283(5)
N(1)-C(16)	1.498(5)	C(18)-C(19)	1.381(6)
N(1)-C(1)	1.517(5)	C(19)-C(20)	1.391(6)
N(2)-C(7)	1.479(6)	C(20)-O(1)	1.280(4)
N(2)-C(5)	1.511(5)	C(20)-C(21)	1.489(5)
N(3)-C(8)	1.496(5)	Cl(1)-O(5)	1.346(8)
N(3)-C(9)	1.519(5)	Cl(1)-O(6)	1.357(7)
N(4)-C(15)	1.502(5)	Cl(1)-O(4)	1.388(7)
N(4)-C(13)	1.502(5)	Cl(1)-O(3)	1.453(5)
C(1)-C(3)	1.527(7)	Cl(2)-O(8)	1.124(12)
C(1)-C(4)	1.531(6)	Cl(2)-O(8)#1	1.124(12)
C(1)-C(2)	1.533(6)	Cl(2)-O(7)#1	1.320(7)
C(4)-C(5)	1.529(7)	Cl(2)-O(7)	1.320(8)
C(5)-C(6)	1.535(6)	Cl(3)-O(9)#2	1.341(5)
C(7)-C(8)	1.486(7)	Cl(3)-O(9)	1.341(5)
C(9)-C(11)	1.525(6)	Cl(3)-O(10)	1.442(7)
C(9)-C(10)	1.530(6)	Cl(3)-O(10)#2	1.442(7)

Table 21. Selected Bond Angles (°) for *cis*-[Cr([14]-decane)-(acac)]$(ClO_4)_2 \cdot 0.5H_2O$

O(2)-Cr(1)-O(1)	89.85(11)	C(7)-N(2)-C(5)	112.0(3)
O(2)-Cr(1)-N(4)	172.94(12)	C(7)-N(2)-Cr(1)	104.5(3)
O(1)-Cr(1)-N(4)	85.34(11)	C(5)-N(2)-Cr(1)	117.2(2)
O(2)-Cr(1)-N(2)	86.46(12)	C(8)-N(3)-C(9)	112.9(3)
O(1)-Cr(1)-N(2)	174.56(12)	C(8)-N(3)-Cr(1)	105.8(2)
N(4)-Cr(1)-N(2)	98.69(12)	C(9)-N(3)-Cr(1)	122.5(2)
O(2)-Cr(1)-N(1)	100.60(12)	C(15)-N(4)-C(13)	110.5(3)
O(1)-Cr(1)-N(1)	87.44(11)	C(15)-N(4)-Cr(1)	104.4(2)
N(4)-Cr(1)-N(1)	84.37(12)	C(13)-N(4)-Cr(1)	118.0(2)
N(2)-Cr(1)-N(1)	89.31(13)	N(1)-C(1)-C(3)	111.4(4)
O(2)-Cr(1)-N(3)	86.98(12)	N(1)-C(1)-C(4)	110.3(3)
O(1)-Cr(1)-N(3)	99.95(12)	C(3)-C(1)-C(4)	108.6(4)
N(4)-Cr(1)-N(3)	88.76(12)	N(1)-C(1)-C(2)	107.0(3)
N(2)-Cr(1)-N(3)	83.86(13)	C(3)-C(1)-C(2)	107.7(4)
N(1)-Cr(1)-N(3)	169.49(12)	C(4)-C(1)-C(2)	111.9(4)
C(16)-N(1)-C(1)	111.6(3)	C(5)-C(4)-C(1)	118.7(4)
C(16)-N(1)-Cr(1)	106.5(2)	N(2)-C(5)-C(4)	110.6(4)
C(1)-N(1)-Cr(1)	122.9(2)	N(2)-C(5)-C(6)	110.9(4)

Table 21. *Continued*

C(4)-C(5)-C(6)	109.8(4)	C(19)-C(18)-C(17)	119.8(4)
N(2)-C(7)-C(8)	109.5(4)	C(18)-C(19)-C(20)	124.2(3)
C(7)-C(8)-N(3)	109.7(4)	O(1)-C(20)-C(19)	124.5(3)
N(3)-C(9)-C(11)	108.6(3)	O(1)-C(20)-C(21)	115.8(3)
N(3)-C(9)-C(10)	108.0(4)	C(19)-C(20)-C(21)	119.7(3)
C(11)-C(9)-C(10)	111.3(4)	C(20)-O(1)-Cr(1)	128.3(2)
N(3)-C(9)-C(12)	109.4(3)	C(18)-O(2)-Cr(1)	128.0(2)
C(11)-C(9)-C(12)	111.3(4)	O(5)-Cl(1)-O(6)	109.2(7)
C(10)-C(9)-C(12)	108.3(4)	O(5)-Cl(1)-O(4)	91.3(7)
C(13)-C(12)-C(9)	119.5(3)	O(6)-Cl(1)-O(4)	118.8(7)
N(4)-C(13)-C(12	111.8(4)	O(5)-Cl(1)-O(3)	107.5(6)
N(4)-C(13)-C(14)	111.5(4)	O(6)-Cl(1)-O(3)	117.7(5)
C(12)-C(13)-C(14)	109.5(4)	O(4)-Cl(1)-O(3)	108.6(4)
C(16)-C(15)-N(4)	109.2(3)	O(8)-Cl(2)-O(8)#1	110(3)
N(1)-C(16)-C(15)	110.4(3)	O(8)-Cl(2)-O(7)#1	116.6(11)
O(2)-C(18)-C(19)	124.9(3)	O(8)#1-Cl(2)-O(7)#1	102.3(14)
O(2)-C(18)-C(17)	115.3(4)		

4) Crystal Structure of *cis*-[{Cr([14]-decane)(μ-cit)}$_2$](ClO$_4$)$_2$ · 6H$_2$O

The structure of the *cis*-[{Cr([14]-decane)(μ-cit)}$_2$](ClO$_4$)$_2$ · 6H$_2$O with the atomic labeling was depicted in Fig. 42. The figure was drawn by ORTEP program at 30% probability level. Table 22 and 23 showed the selected bond distances and bond angles. The structure of the cation in this complex revealed two identical homobinuclear Cr(III)Cr(III) cores joined by two bridging cit(-OOCCH$_2$C-(OH)(CH$_2$COOH)COO-) group linkage. The cation was centro-symmetric. The structure analysis indicated that the crystal consists of di(μ-cit){([14]-decane)chromium(III)}$_2$ cation([4]) and perchlorate in a molecular ratio of 1:2, so that it can be formulated as *cis*-[{Cr([14]-decane)(μ-cit)}$_2$](ClO$_4$)$_2$ · 6H$_2$O. This was well fitted with elemental analysis and molar conductivity (168.6 ohm^{-1} cm^2 mol^{-1}). The hexacoordination geometry around Cr(III) ion was a distorted octahedral {CrN$_2$O$_2$(*O-cit*)-plane and two macrocyclic N (*C-dimethyl*) group of its z-axis} in which Cr(III) was coordinated with the four secondary nitrogen atoms of the macrocycle as well as with two oxygen atom of two monodentated citrate in the *cis* position. The average Cr-N bond distance was 2.121(9)Å and the average Cr-O bond distance was 1.958(8)Å. These values were similar to acetylactonate and *p*-chlorobenzonate Cr(III) complexes of [14]-decane. The Cr-N (*C-dimethyl*) bond distances {Cr-N(2); 2.147(9)Å, Cr-N(4); 2,117(9)Å} were slightly longer (average 0.022 Å) than the Cr-N (*C-methyl*) bond distances {Cr-N(1); 2.108(9)Å, Cr-N(3); 2,111(9)Å}. The bond angles with the metal ion revealed distorted octahedral structure: O(1)-Cr-N(1) and O(3)-Cr-N(3) angles are 86.8(3)° and 84.8(4)°, respectively.

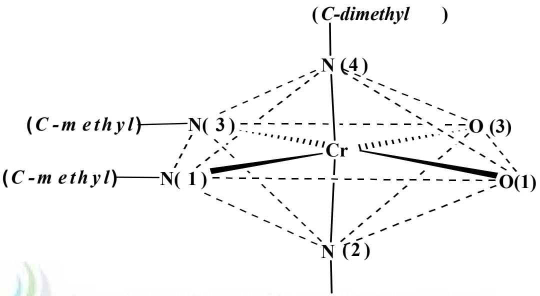

The distence between two Cr metal ions was 7.360Å. In this complex also had intramolecular hydrogen bond, similar with p-chlorobenzoic acid case. Interactions between the uncoordinated carboxylate oxygen atoms of citrate and the hydrogen atom of secondary amines in macrocycle formed stable six-membered rings.

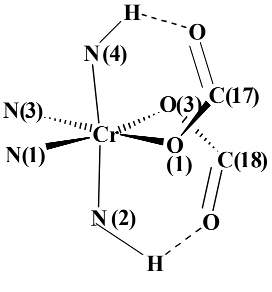

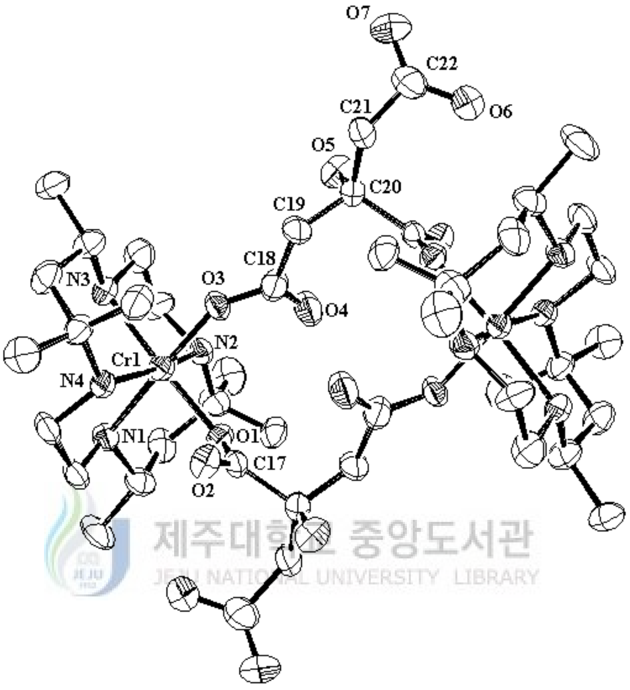

Fig. 42. ORTEP plot of the *cis*-[{Cr([14]-decane)(μ-cit)}$_2$](ClO$_4$)$_2$ · 6H$_2$O complex.

Table 22. Selected Bond Lengths (Å) for *cis*-$[\{Cr([14]\text{-decane})(\mu\text{-cit})\}_2](ClO_4)_2 \cdot 6H_2O$

Cr(1)-O(3)	1.942(8)	C(11)-C(12)	1.54(2)
Cr(1)-O(1)	1.974(8)	C(12)-C(13)	1.50(2)
Cr(1)-N(1)	2.108(9)	C(12)-C(14)	1.56(2)
Cr(1)-N(3)	2.111(9)	C(15)-C(16)	1.51(2)
Cr(1)-N(4)	2.117(9)	C(17)-O(2)	1.237(14)
Cr(1)-N(2)	2.147(9)	C(17)-O(1)	1.28(2)
N(1)-C(16)	1.494(14)	C(17)-C(20)#1	1.54(2)
N(1)-C(1)	1.54(2)	C(18)-O(4)	1.23(2)
N(2)-C(7)	1.49(2)	C(18)-O(3)	1.314(14)
N(2)-C(4)	1.55(2)	C(18)-C(19)	1.52(2)
N(3)-C(8)	1.503(14)	C(19)-C(20)	1.49(2)
N(3)-C(9)	1.51(2)	C(20)-O(5)	1.41(2)
N(4)-C(15)	1.501(14)	C(20)-C(21)	1.50(2)
N(4)-C(12)	1.50(2)	C(20)-C(17)#1	1.54(2)
C(1)-C(2)	1.51(2)	C(21)-C(22)	1.52(2)
C(1)-C(3)	1.53(2)	C(22)-O(7)	1.21(2)
C(3)-C(4)	1.53(2)	C(22)-O(6)	1.27(2)
C(4)-C(5)	1.50(2)	Cl(1)-O(11)	1.345(13)
C(4)-C(6)	1.53(2)	Cl(1)-O(8)	1.378(13)
C(7)-C(8)	1.50(2)	Cl(1)-O(9)	1.394(13)
C(9)-C(11)	1.51(2)	Cl(1)-O(10)	1.42(2)
C(9)-C(10)	1.55(2)		

Table 23. Selected Bond Angles (°) for *cis*-[{Cr([14]-decane)(μ-cit)}$_2$](ClO$_4$)$_2$ · 6H$_2$O

O(3)-Cr(1)-O(1)	90.4(3)	C(7)-N(2)-Cr(1)	104.5(7)
O(3)-Cr(1)-N(1)	177.2(4)	C(4)-N(2)-Cr(1)	122.9(8)
O(1)-Cr(1)-N(1)	86.8(3)	C(8)-N(3)-C(9)	109.4(10)
O(3)-Cr(1)-N(3)	84.8(4)	C(8)-N(3)-Cr(1)	105.5(6)
O(1)-Cr(1)-N(3)	174.8(4)	C(9)-N(3)-Cr(1)	117.6(7)
N(1)-Cr(1)-N(3)	98.0(4)	C(15)-N(4)-C(12)	113.2(9)
O(3)-Cr(1)-N(4)	96.6(3)	C(15)-N(4)-Cr(1)	107.8(7)
O(1)-Cr(1)-N(4)	92.0(4)	C(12)-N(4)-Cr(1)	123.4(7)
N(1)-Cr(1)-N(4)	83.7(4)	C(2)-C(1)-C(3)	109.2(11)
N(3)-Cr(1)-N(4)	86.6(4)	C(2)-C(1)-N(1)	112.4(10)
O(3)-Cr(1)-N(2)	92.4(3)	C(3)-C(1)-N(1)	110.0(10)
O(1)-Cr(1)-N(2)	98.1(4)	C(4)-C(3)-C(1)	119.7(11)
N(1)-Cr(1)-N(2)	87.8(4)	C(5)-C(4)-C(3)	108.8(12)
N(3)-Cr(1)-N(2)	84.1(4)	C(5)-C(4)-C(6)	108.0(11)
N(4)-Cr(1)-N(2)	166.4(4)	C(3)-C(4)-C(6)	113.0(11)
C(16)-N(1)-C(1)	110.3(9)	C(5)-C(4)-N(2)	111.7(11)
C(16)-N(1)-Cr(1)	105.4(7)	C(3)-C(4)-N(2)	109.2(10)
C(1)-N(1)-Cr(1)	116.9(7)	C(6)-C(4)-N(2)	106.2(10)
C(7)-N(2)-C(4)	113.3(10)	N(2)-C(7)-C(8)	111.6(11)

Table 23. *Continued*

C(7)-C(8)-N(3)	106.8(11)	C(20)-C(19)-C(18)	117.2(11)
N(3)-C(9)-C(11)	109.6(10)	O(5)-C(20)-C(19)	109.8(10)
N(3)-C(9)-C(10)	112.2(10)	O(5)-C(20)-C(21)	107.4(11)
C(11)-C(9)-C(10)	110.2(10)	C(19)-C(20)-C(21)	109.0(10)
C(9)-C(11)-C(12)	119.4(9)	O(5)-C(20)-C(17)#	109.7(11)
C(13)-C(12)-N(4)	108.8(9)	C(19)-C(20)-C(17)#	109.5(10)
C(13)-C(12)-C(11)	113.0(11)	C(21)-C(20)-C(17)#	111.4(10)
N(4)-C(12)-C(11)	108.4(10)	C(20)-C(21)-C(22)	117.2(12)
C(13)-C(12)-C(14)	108.9(11)	O(7)-C(22)-O(6)	126(2)
N(4)-C(12)-C(14)	110.5(10)	O(7)-C(22)-C(21)	121.3(14)
C(11)-C(12)-C(14)	107.3(9)	O(6)-C(22)-C(21)	113(2)
N(4)-C(15)-C(16)	108.9(9)	O(11)-Cl(1)-O(8)	114.6(10)
N(1)-C(16)-C(15)	109.1(10)	O(11)-Cl(1)-O(9)	113.8(9)
O(2)-C(17)-O(1)	126.7(11)	O(8)-Cl(1)-O(9)	107.2(11)
O(2)-C(17)-C(20)#	117.9(14)	O(11)-Cl(1)-O(10)	107.8(13)
O(1)-C(17)-C(20)#	115.4(12)	O(8)-Cl(1)-O(10)	99.9(13)
O(4)-C(18)-O(3)	124.2(12)	O(9)-Cl(1)-O(10)	112.8(12)
O(4)-C(18)-C(19)	122.5(12)	C(17)-O(1)-Cr(1)	134.1(7)
O(3)-C(18)-C(19)	113.2(11)	C(18)-O(3)-Cr(1)	134.3(8)

IV. Conclusions

The reaction of *cis*-$[Cr([14]\text{-}decane)(OH_2)_2]^+$ ([14]-decane = *rac*-5, 5, 7, 12, 12, 14-hexamethyl-1, 4, 8, 11-teraazacyclotetradecane) with O- {L_a : chloroacetate (ca), benzoate (bz), *p*-chlorobenzoate (cbz), oxalate (ox), malonate (mal), acetylacetonate (acac), citrate (cit)}, or N- {L_a : NCS^-, N_3^-} bonded auxiliary ligands formed a new *cis*-$[Cr(III)([14]\text{-}decane)(L_a)_m]^{n+}$ complexes. The complexes have shown a distorted octahedral coordination environment with the macrocycle adopting a folded *cis*-V conformation.

The structure analysis indicated that the crystal consists of di(isothiocyanato)([14]-decane)chromium(III) mono-cation and perchlorate ion in the molecular ratio of 1:1, formulated as $[Cr([14]\text{-}decane)(NCS)_2]ClO_4 \cdot H_2O$. This was well fitted with elemental analysis results. The hexacoordination geometry around Cr(III) ion exhibited a distorted octahedral structure {$CrN_2N'_2$ (N'-*NCS*)-plane and two N (*C-dimethyl*) group of its z-axis}. In this complex Cr(III) was coordinated with the four secondary nitrogen atoms of the macrocycle and two nitrogen atom of two isothiocyanate in the *cis* position.

The structure analysis revealed the crystal consists of di(*p*-chlorobenzoato)([14]-decane) chromium(III) mono-cation and perchlorate anion in a molecular ratio of 1:1, so formulated as [Cr([14]-decane)(cbz)$_2$]ClO$_4$. This was well fitted with elemental analysis results. The hexacoordination geometry around Cr(III) ion was a distorted octahedral {CrN$_2$O$_2$(*O-cbz*)-plane and two N (*C-dimethyl*) group of its z-axis} in which Cr(III) was coordinated with the four secondary nitrogen atoms of the macrocycle as well as with two oxygen atom of two chlorobezoate in the *cis* position. Intramolecular hydrogen bonding interactions were found between the uncoordinated carboxylate oxygen atoms of *p*-chlorobenzoic acid and the hydrogen atom of secondary amines in the macrocycle formed stable six-membered rings.

In the structure of *cis*-[Cr([14]-decane)(acac)](ClO$_4$)$_2$ · 0.5H$_2$O, the hexacoordination geometry around Cr(III) ion was a distorted octahedral {CrN$_2$O$_2$(*O-acac*)-plane and two N(*C-dimethyl*) group of its z-axis} in which Cr(III) was coordinated with the four secondary nitrogen atoms of the macrocycle as well as with two oxygen atom of bidentated acethylacetone(acac) in the *cis* position.

The structure of the cation in citrato complex revealed two identical homobinuclear Cr(III)Cr(III) cores joined by two bridging citrato group linkage. The cation was centro-symmetric. The structure analysis indicated that the crystal consists of di(μ-cit){([14]-decane)chromium(III)}$_2$ cation([4]) and perchlorate in a molecular ratio of 1:2, so that it can be formulated as *cis*-$[\{Cr([14]\text{-decane})(\mu\text{-cit})\}_2](ClO_4)_2 \cdot 6H_2O$. This was well fitted with elemental analysis and molar conductivity. The hexacoordination geometry around Cr(III) ion was a distorted octahedral {CrN_2O_2(*O-cit*)-plane and two macrocyclic N (*C-dimethyl*) group of its z-axis} in which Cr(III) was coordinated with the four secondary nitrogen atoms of the macrocycle as well as with two oxygen atom of two monodentated citrate in the *cis* position. The distence between two Cr metal ions was 7.360Å. In this complex also had intramolecular hydrogen bond, similar with p-chlorobenzoic acid case. Interactions between the uncoordinated carboxylate oxygen atoms of citrate and the hydrogen atom of secondary amines in macrocycle formed stable six-membered rings.

The visible absorption spectra of *cis*-$Cr([14]\text{-decane})(L_a)_m]^{n+}$ in DMF solution at room temperature exhibited two bands, at 17400~18800 cm^{-1}(ν_1) and 23400~25900 cm^{-1}(ν_2), due to the $^4A_{2g} \rightarrow {}^4T_{2g}$ and $^4A_{2g} \rightarrow {}^4T_{1g}$ (O_h) transitions, respectively. In these complexes, the nearly symmetric profiles of two quartet bands and the higher extinction coefficient of 134~223 M^{-1} cm^{-1} were evidences of the *cis* configuration. A chromium complexes in tetragonal symmetry are expected to have four absorption bands in *d-d* region, but each spectrum apparently has two major components. For the splitting of the two bands, we have fitted the band profiles to four or five Gaussian curves. The contribution from outside bands was corrected for fine deconvolution. The four peak positions can be assigned to the ^4E ($^4T_{2g}$ in O_h symmetry), $^4B_2$ ($^4T_{2g}$), ^4E ($^4T_{1g}$) and $^4A_2$ ($^4T_{1g}$), respectively.

In mid-infrared spectra of the nine complexes, the broadness of absorption bands near 3400 cm^{-1} indicated that there were hydrogen bonds in these complexes. Two strong bands in the region of 3300 ~ 3050 cm^{-1} were due to the symmetric and antisymmetric N-H stretching modes. Two strong bands in the region of 2990 ~ 2860 cm^{-1} were due to the symmetric and antisymmetric C-H stretching modes. The very strong absorption at near 1100 cm^{-1} and near 620 cm^{-1} were assigned to ionic perchlorate. Two peaks at near 440 and near 480 cm^{-1} were assigned to the Cr-N stretching mode. The present complexes exhibited three N-H wagging bands at near 890, near 860 and near 840 cm^{-1} region. Two CH_2 rocking bands were exhibited at near 820 and near 780 cm^{-1}. Since the infrared spectra of the title complexes were consistent with the *cis* configuration. The IR spectra of the *cis*-[Cr([14]-decane)$(NCS)_2$]ClO_4 complex revealed that the ambidentate thiocyanate ligand was N-bonded. Two stretching frequencies ν_{as} (COO^-) and ν_s (COO^-) found at near 1600 and near 1350 cm^{-1} revealed that the carboxylate oxygen was coordinated. Unidentate carboxylate complexes have much greater $\Delta\nu$ [between $\nu_{as}(COO^-)$ and $\nu_s(COO^-)$] values than the ionic compounds. Since there were large $\Delta\nu$ values (oxalate: 296 cm^{-1}, malonate: 296 cm^{-1}, bezonate: 242 cm^{-1}, p-chlorobezonate: 257 cm^{-1}, chloroacetate : 338 cm^{-1}, citratate: 230 cm^{-1}), carboxylates coordinated as unidentate.

The FAB mass spectra peaks of all complexes were corresponding to the molecular ion $[Cr([14]\text{-decane})(L_a)_m]^+$ (m = 1 or 2). The complexes of two coordinated auxiliary ligands generated two peaks to the species $[Cr([14]\text{-decane})(L_a)]^+$ and $[Cr([14]\text{-decane})(L_a)_2]^+$ {NCS^- : *m/z* 394, 452 ; N_3^- : 377, 420 ; benzonate (bz) : *m/z* 456, 578 ; *p*-chlorobenzonate (cbz) : *m/z* 490, 646 ; chloroacetate (ca) : *m/z* 428, 522 }.

Thermogravimetry analysis(TGA) for the Cr(III) complexes of [14]-decane ligand was found out from the results that the prepared macrocycle compounds have relatively high thermal stability. The macrocyclic entity changed slowly up to 350℃, and then those complexes have been changed to green Cr_2O_3 were observed at over 990℃.

Reference

1. Poonia, N. S. ; Bajaj, A. V., *Chem. Rev* 1979, 79, 389.
2. Bajaj, A. V. ; Poonia, N. S., *Coord. Chem. Rev* 1988, 87, 55.
3. Izatt, R. M. ; Bradshaw, J. S. ; Christensen, J. J., *Chem. Rev* 1985, 85, 271.
4. Cabbiness, D. K. ; Margerum, D. W., *J. Am. Chem. Soc.* 1969, 91, 6540.
5. Hinz, F. P. ; Margerum, D. W., *Inorg. Chem.* 1974, 13, 2941.
6. Hinz, F. P. ; Margerum, D. W. *J. Am. Chem. Soc.* 1974, 96, 4993.
7. Fabbrizzi, L. ; Paoletti, P. ; Clay, R. M., *Inorg. Chem.* 1978, 17, 1042.
8. Kodama, M. ; Kimura, E. ; *J. Chem. Soc. Dalton Trans.* 1978, 247.
9. Smith, G. F. ; Margerum, D. W., *J. Chem. Soc. Chem. Commum.* 1975, 807.
10. Chock, P. B. ; Titus, E. O., *Prog. Inorg. Chem.* 1973, 18, 287.
11. Thöm, V. J. ; Hancock, R. D., *J. Chem. Soc. Dalton Trans.* 1985, 1877.
12. Martin, L. Y. ; DeHayes, L. J. ; Busch, D. H., *J. Am. Chem. Soc.* 1974, 96, 4047.

13. Grootenhuis, P. D. J. ; Reinhoudt, D. N., *Tetrahedron* **1987**, 43, 397.

14. Bradshaw, J. S. ; Mass, G. E. ; Christensen, J. J., *J. Am. Chem. Soc.* **1980**, 102, 467.

15. Kumar, S. ; Kaur, N. ; Singh, H., *Tetrahedron Lett.* **1996**, 37, 2071.

16. Sherry, A. D., *J. Less-Common Metals* **1989**, 149, 133.

17. Wu, S. L. ; Jr. Horrocks, W. D., *Inorg. Chem.* **1995,** 34, 3724.

18. Sherry, A. D. ; Geraldes, C. F. G. C., *Lanthanide Probes in Life, Chemical and Earth Sciences, Theory and Practice* ; Bunzli, J. C. G. ; Choppin, G. R., Eds ; Elsevier : Amsterdam, **1989** ; Chapter 4.

19. Jurisson, S. ; Berning, D. ; Jia, W. ; Ma, D., *Chem. Rev*. **1993**, 93, 1137.

20. Wang, X. ; Jin, T. ; Combin V. ; Lopez-Mut, A. ; Merciny, E. ; Desreux, J. F. , *Inorg. Chem.* **1992**, 31, 1095.

21. Runge, V. M. *Enhenced Magnetic Resonance Imaging* ; C. V. Mosby Co. ; St. Louis, MO, **1989**.

22. Lázár, I ; Hrncir, D. C. ; Kiefer, G. E. ; Sherry, A. D., *Inorg. Chem.* **1992**, 31, 4422.

23. Geiger, D. K. ; Pavlak, E. J. ; Kass, L. T., *J. Chem. Educ.* **1991**, 68, 337.

24. Balducci, G. ; Savéant, J. M., *Inorg. Chem.* **1994**, 33, 1972.

25. Houeto, P. ; Borron, S. W. ; Sandouk, P. ; Baud, F. J., *J. Toxicol. Clin. Toxicol.* **1996**, 34, 397.

26. Houto, P. ; Buneaux, F. ; Baud, F. J. ; Levillain, P., *J. Anal. Toxicol.* **1994**, 18, 154.

27. McGuinn, W. D. ; Baxter, L. ; Cannon, E. P. ; Way, J. L., *Fundam, Appl. Toxicol.* **1994**, 23, 76.

28. Curtis, N. F., *J. Chem. Soc.* **1964**, 2644.

29. Eriksen, J. ; Monsted, O., *Acta Chem. Scand.* **1983**, A37 , 579.

30. Sheldrick, G. M. *SHELXL-97, Program for the Refinement of Crystal Structures*; University of Göttingen : Germany, **1997**.

31. House, D. A. ; Hay, R. W. ; Ali, M. A., *Inorg. Chim. Acta* **1983**, 72, 239.

32. Dubicki, L..; Day, P. *Inorg. Chem.* **1971**, 10, 2043.

33. Swisher, R. G.; Brown, R. C.; Smierciak, R. C.; Blinn, E. L. *Inorg. Chem.* **1981**, 20, 3947.

34. Ferguson, J. ; Tobe, M. L., *Inorg. Chim. Acta* **1970**, 4, 109.

35. MacDonald D. J. ; Garner, C. S. , *J. Am. Chem. Soc.* **1961**, 83, 4252.

36. Woldbye F. , *Acta Chem. Scand.* 1958, 12, 1079.

37. Nakamoto, K. *Infrared and Raman Spectra of Inorganic and Coordination Compounds*, Part B ; John Wiley & Sons ; New York, **1997**.

38. Choi, J. H. *Spectrochim. Acta* 2000, 56A, 1653.

39. Choi, J. H. *Chem. Phys.* 2000, 256, 29.

40. Poon, C. K. ; Pun, K. C., *Inorg. Chem.* 1980, 19, 568.

41. Chan, P. K. ; Poon, C. K., *J. Chem. Soc. Dalton Trans.* 1976, 858.

42. Goedken, V. L. ; Merrell, P. H. ; Busch, D. H. , *J. Am. Chem. Soc.* 1972, 94, 3397.

43. Meyer, K. ; Bendix, J. ; Metzler-Nolte, N. ; Weyhermuller, T. ; Weighardt, K., *J. Am. Chem. Soc.* 1998, 120, 7260.

44. Choi, J. H. ; Suzuki, T. ; Subhan, Md. A. ; Kaizaki, S. ; Park, Y. C., *Acta Cryst.* 2002, *C58,* m409.

45. Choi, J. H. ; Suh, I. H. ; Kwak, S. H., *Acta Cryst.* 1995, *C51*, 1745.

46. Choi, J. H. ; Suzuki, T. ; Kaizaki, S., *Acta Cryst.* 2002, *C58*, m539.

국문초록

cis-$[Cr([14]\text{-decane})(OH_2)_2]^+$ ([14]-decane = *rac*-5, 5, 7, 12, 12, 14-hexamethyl-1, 4, 8, 11-teraazacyclotetradecane)와 O-주게 리간드 {L_a : chloroacetate, benzoate, *p*-chlorobenzoate, oxalate, malonate, acetylacetonate, citrate} 또는 N-주게 보조 리간드 {L_a : NCS^-, N_3^-}의 반응으로부터 새로운 *cis*-$[Cr(III)([14]\text{-decane})(L_a)_m]^{n+}$ 착물을 합성하였다. 이들 착물들은 원소분석, 전기전도도, UV-Vis, IR 분광법, 질량 분석법, 열중량 분석법 및 X-ray 결정분석법 등을 이용하여 특성 및 구조적 성질을 확인·고찰하였다. 이들 착물들은 보조 리간드가 *cis*-V형으로 결합된 찌그러진 팔면체 구조를 이루고 있음을 확인하였다. isothiocyanate 및 *p*-chlorobenzonate 착물들은 2개의 보조 리간드가 Cr^{3+} 중심금속에 monodentate로 배위된 *cis*-$[Cr([14]\text{-decane})(NCS)_2]ClO_4 \cdot H_2O$과 *cis*-$[Cr([14]\text{-decane})(cbz)_2]ClO_4$ 착물을 형성하였다. acetylacetonate 착물은 1개의 보조 리간드가 Cr^{3+} 중심금속에 bidentate로 배위된 *cis*-$[Cr([14]\text{-decane})(acac)](ClO_4)_2 \cdot 0.5H_2O$ 착물을 형성하였다. 또한, citrate 착물은 2개의 citrate가 2개의 Cr^{3+}에 다리로 배위된 *cis*-$[\{Cr([14]\text{-decane})(\mu\text{-cit})\}_2](ClO_4)_2 \cdot 6H_2O$ 착물을 형성하였고, 두 금속간의 거리는 7.360Å이었다. DMF 용액에서 Cr 착물들의 전자흡수 스펙트럼 결과, $^4A_{2g} \rightarrow {}^4T_{2g}$와 $^4A_{2g} \rightarrow {}^4T_{1g}$ (O_h) 전이에 해당하는 17400～18800 cm^{-1}(ν_1) 와 23400～25900 cm^{-1}(ν_2)에 흡수띠가 나타났다. Cr 착물들의 FAB 질량 분석에서 $[Cr([14]\text{-decane})(L_a)_m]^+$ 착이온 종에 해당하는 피이크들을 확인할 수

있었다. 열중량 분석 결과 착물들은 비교적 열적으로 안정하였으며, 350℃ 이상에서 거대고리 리간드가 서서히 분해가 일어나 최종적으로 990℃ 이상에서는 녹색의 Cr_2O_3로 변해감을 확인하였다.

감사의글

짧지 않은 시간이었습니다.
여러모로 부족한 저를 지금까지 이끌어 주신 변종철 교수님을 비롯하여 늘 격려해 주시고 용기를 북돋워 주신 제주대학교 화학과 교수님들 한분 한분께 깊이 감사드립니다. 또한, 먼 길을 마다 않으시고 제주까지 와 주셔서 깨우침과 자상한 지도를 해주신 박유철 교수님과 김양 교수님께 다시 한번 머리 숙여 감사드립니다. 이것이 끝이 아니고 단지 새로운 시작을 위한 작은 매듭임을 깨닫게 해 주심 감사드립니다.

멋모르고 욕심만 내어 시작하였다가 중도에 어찌할 바 모르고 방황도 하였습니다. 그때마다 주위의 여러분들이 격려해 주신 덕분에 여기까지 올 수 있었습니다.

이 매듭을 짓는데 있어서 가장 큰 도움을 준 한충훈 학우, 문대훈 선생님, 이우환 선생님과 제주대 무기화학연구실 후배 모두에게 각별한 감사를 드리며, 모두 건승하시길 바랍니다.

묵묵히 옆에서 늘 믿어주고 도와준 아내와 두 아들 원영, 원재 세상 누구보다 사랑합니다. 평생을 고생하시는 부모님께 늘 마음이 무거웠습니다. 이 일이 부모님께 작은 기쁨이라도 되기를 바랍니다.

지금껏 살아오는 동안 여러 장소 여러 가지에 걸친 수많은 인연들을 소중하게 생각합니다. 일일이 열거하지 못한 모든 인연들이 모두 합하여 큰 선을 이루게 되기 바랍니다.

끝으로 제주대로의 첫 발을 내 딛던 날 먼 나라로 가신 장인어른과 제가 나서 철 들 때까지 오로지 한마음으로 보살펴 주신 할머님이 그립습니다.